5-2012

Temperature Effects On Integral Abutment Bridges For The Long-Term Bridge Performance Program

Leo E. Rodriguez
Utah State University

TEMPERATURE EFFECTS ON INTEGRAL ABUTMENT BRIDGES FOR THE LONG-TERM BRIDGE PERFORMANCE PROGRAM

by

Leo E. Rodriguez

A thesis submitted in partial fulfillment
of the requirements for the degree

of

MASTER OF SCIENCE

in

Civil and Environmental Engineering

Approved:

_____	_____
Paul J. Barr Major Professor	Marvin W. Halling Committee Member
_____	_____
Joseph A. Caliendo Committee Member	Mark R. McLellan Vice President for Research and Dean of the School of Graduate Studies

UTAH STATE UNIVERSITY
Logan, Utah

2012

ABSTRACT

Temperature Effects on Integral Abutment Bridges for

The Long-Term Bridge Performance Program

by

Leo E. Rodriguez, Master of Science

Utah State University, 2012

Major Professor: Dr. Paul J. Barr
Department: Civil and Environmental Engineering

The United States Department of Transportation (US-DOT) Federal Highway Administration (FHWA) initiated in 2009 the Long-Term Bridge Performance (LTBP) program to gather high-quality data on a representative sample of bridges over a twenty-year period of time. The goal of this program is to quantify how bridges behave during their service life while being exposed to different types of loadings and deterioration due to corrosion, fatigue and various climate conditions along with their corresponding maintenances. The data gathered will result in the creation of databases of high quality data, acquired through long-term instrumentation, to be used for improved design practices and effective management of infrastructures by employing best practices for maintenance. As part of the LTBP Program two integral abutment bridges, a California Bridge near Sacramento, CA and a Utah Bridge near Perry, UT, were selected to be monitored for

temperature changes as well as to undergo periodic live-load testing. Live-load testing included slowly driving a truck over the bridges.

The bridges were instrumented to collect test data and use it to calibrate a finite-element model. This finite-element model was used to determine the actual bridge behavior and compare it with the AASHTO LRFD Specifications.

This thesis also examined how different parameters such as thermal gradients, mean temperature, and end-rotation affect these two integral abutment bridges.

(81 pages)

PUBLIC ABSTRACT

Temperature Effects on Integral Abutment Bridges for the Long-Term Bridge Performance Program

The Long-Term Bridge Performance (LTBP) program was started by the Federal Highway Administration (FHWA) in 2009 to gather high-quality data on a collection of typical bridges over a twenty-year period of time. The goal of this program is to create databases of high quality data acquired through long-term instrumentation of the bridges behavior during their service life.

The data gathered will be used to improve design practices and effective management of infrastructures. As part of the LTBP Program two integral abutment bridges, a California Bridge near Sacramento, CA and a Utah Bridge near Perry, UT, were selected to be monitored for temperature changes as well as to undergo periodic live-load testing. Live-load testing included slowly driving a truck over the bridges.

The bridges were instrumented to collect test data and use it to calibrate a finite-element model. This finite-element model was used to determine the actual bridge behavior and compare it with the AASHTO LRFD Specifications.

Leo E. Rodriguez

ACKNOWLEDGMENTS

First, I would like to thank my major professor, Dr. Paul Barr, for his guidance, encouragement and constant support throughout the time I've been at Utah State University and especially on this project. I would also like to express my appreciation to Dr. Marvin Halling and Dr. Joseph Caliendo for their guidance and support during this project. The three of you are a great example of what a professor should be and are definitely role models for this institution. Also, I would like to thank Steven Petroff, who was always willing to help, guide and provide me with the necessary tools to continue with my research. His help was a key factor for my thesis work.

I would also like to thank my family for always being there to support me, give me strength and encourage me to continue with my education and to accomplish all of my desired goals. You have provided me with infinite love in spite of the great distance that separates us. I also want to thank my friends back home and at USU for always being there. Last but not least, I would like to thank you for your constant love and support. Even though our lives have been a constant roller-coaster ride, I will keep enjoying it because it gives the most needed adrenaline my life needs every day to survive.

Leo E. Rodriguez

CONTENTS

Page

LIST OF FIGURES

Figure Page

LIST OF EQUATIONS

LIST OF NOTATIONS

Ai……Area of the bridge cross section of the *i*-th segment;

Ei……Modulus of elasticity of the cross section of the i-th segment;

f'_c ……Specified compressive strength;

f_r ……The modulus of rupture for concrete;

T_{avg}……Average of the bridge temperature over the bridge cross section;

$T_{avg\text{-}min}$…Minimum Average of the bridge temperature over the bridge cross section;

$T_{avg\text{-}max}$…Maximum Average of the bridge temperature over the bridge cross section;

T_i……Temperature of the cross section of the *i*-th segment;

α_i……Coefficient of thermal expansion of the material used for the *i*-th segment;

CHAPTER 1

INTRODUCTION

Organization

The organization of this thesis is as follows:

Chapter 2. Chapter 2 presents a summary of research that has been done in the field of temperature studies, monitoring and finite-element modeling of various bridge structures.

Chapter 3. Chapter 3 describes the dimensions and properties of the California and Utah Bridges. It also gives a description of the live-load testing conducted. After the brief description of live-load testing, the chapter further goes on to present the measured results of the finite-element due to temperature and a comparison with the field data obtained.

Chapter 4. Chapter 4 is a summary of the thesis content along with several conclusions made about important bridge behaviors and predictions of the California and Utah Bridge.

Preface

The inclusion of temperature effects for concrete bridges has traditionally been incorporated in design by allowing for expansion and contraction through the utilization of bearings and joints. However, as a result of the growth in the multi-modal transportation system, more complex and longer spans bridges are now being constructed, requiring new material technologies and design methodologies causing the accurate accounting of thermal loading to become more crucial. A nonlinear temperature distribution through the bridge cross section is caused by the relatively low thermal conductivity of the concrete and the variation of temperature magnitudes with time. This nonlinear temperature distribution induces stresses in the transverse and longitudinal directions that can lead to cracking and unacceptable service conditions.

Temperature gradients that are produced on a bridge structure during service depend mainly on geometry, location and orientation, bridge properties and conditions, environment and during construction the heat of hydration of the concrete and placement of an asphalt overlay. Imprecise thermal analysis of bridges has led to severe cracking and failure of structures (; Leonhardt 1970; Priestley 1978; Imbsen 1985; Moorty and Roeder 1990). To address these observed durability issues, engineers have, at times, reduced the number of joints and designed monolithic cast-in-place structures such as integral abutment bridges. The thermal movement of these bridge types are restrained therefore proper calculation and detailing of the inherent stresses are essential.

Several theoretical relationships based on one- and two-dimensional heat flow theory, solar radiation levels and daily air temperature distribution have been proposed to predict the changes in the nonlinear temperature distribution over a typical bridge cross section. Although the exact procedures for these proposed relationships vary, the objective is to obtain a better estimate of the temperature and stress distribution (Roeder 2003). Thepchatri and Johnson (1978) proposed a method to obtain temperature effects for various types of highway bridge cross sections and different environmental conditions by using a finite-element analyses that also incorporated heat flow and thermal analysis validated by the similarity in predicted and measured data. Priestley et al. (1984) developed a thermal design procedure based on a research conducted in New Zealand. The overall design philosophy consisted of three procedures outlined as follows: First, prediction of the critical design gradient based on known local ambient characteristics. Second, calculation of the corresponding stress levels based on simple statics induced in the bridge superstructure by the design thermal gradient. Third, quantify the influence of the thermally induced stresses for serviceability and ultimate load states. This procedure served as a basis for the development of a linear standard thermal design gradient that was adopted in the AASHTO Specifications.

Roeder (2003) proposed an alternative method for determining bridge design temperatures and thermal movements. For this research, 1,273 temperature measurements with an average time history of 70.7 years from different locations in the United States were utilized. This diverse data set resulted in the creation of temperature design maps for concrete and steel bridges with concrete decks for the

continental 48 states. This method was adopted by the AASHTO LRFD Specifications in 2005 as an alternative to methods proposed by other researchers. Other studies that have quantified the temperature effects on bridges include Emerson (1982) and Branco and Mende (1993).

For this research, the temperature response of two integral abutment bridges (one in California and the other in Utah) were monitored for approximately one year using a dense array of thermocouples throughout the depth of the bridge deck and over the height of the girders. Changes in concrete temperatures were recorded resulting in maximum and minimum average values in addition to temperature gradients. Validated finite-element models (FEM) based on changes in strain and deflections monitored during live-load test for the California Bridge and changes in rotations from the measured thermal gradients on the Utah Bridge were used to predict bridge internal stresses due to measured temperature variations throughout the cross section of the bridge models. Due to the significant measured end restraint (especially from the California Bridge) from the integral abutments, these validated models provided a more accurate representation of the bridge behavior at the service state. As a result, tensile stresses and temperature differential were obtained and were compared with calculated values in accordance to current design specifications.

CHAPTER 2

LITERATURE REVIEW

The Long-Term Bridge Performance (LTBP) program was initiated in 2009 by the United State Department of Transportation (US-DOT) Federal Highway Administration (FHWA) with the focus of gathering high-quality data on a representative sample of bridges over a twenty year period of time. The goal of this program is to quantify how bridges behave during their service life while being exposed to different types of loadings and deterioration due to corrosion, fatigue and various climate conditions along with their corresponding maintenances. The data gathered will result in the creation of databases of high quality data, acquired through long-term instrumentation, to be used for improved design practices, effective management of infrastructures by employing best practices for maintenance. As part of the LTBP Program two integral abutment bridges, a California Bridge near Sacramento, CA and a Utah Bridge near Perry, UT were selected to be monitored for temperature changes as well as to undergo periodic live-load testing. Live-load testing included slowly driving a truck over the bridges on selected load paths. The data collected was analyzed and used to calibrate a finite-element model. Until a good correlation between the recorded test data and finite-element models was obtained. Based on the good correlation between the finite-element models and test data, it was concluded that the finite-element models accurately predicted the actual bridge behaviors. From these finite-element models the overall performance due to temperature loadings were quantified.

Integral abutment bridges have gained popularity as low maintenance alternatives by elimination of the expansion joints. However, with the increasing use of monolithic systems with restrained members, it has resulted in a potentially serious environmentally-induced effect associated with vertical temperature gradient through member cross-sections induced by solar radiation and ambient temperature variation (i.e. Priestley 1978; Roeder 2003). As a result of these temperature variations, horizontal movements and tensile stresses are induced in both statically determinate and indeterminate bridges.

Since, bridge movements are controlled by the average temperature over its cross section (Roeder 2003), a significant amount of data was collected for both the California and Utah Bridges and was compared to the maximum and minimum design recommendation maps provided in the AASHTO LRFD Specifications (2010). This map showed that bridges can often be designed for smaller movements than required by the AASHTO Specifications (1996). The maximum and minimum average temperatures of the California and Utah Bridges were predicted with 17 % and 27%, respectively.

According to Elbadry and Ghali (1986), in statically determinate bridges, non-linear temperature distribution produce stresses in the longitudinal direction that are self-equilibrating and no variations in reactions occur. In statically indeterminate bridges, the curvature due to temperature will be restrained and statically indeterminate reactions and continuity moments are developed. Therefore, the continuity stresses that are produced are added to the self-equilibrating stresses to obtain the total thermal induced stresses. For the California Bridge, which acts as statically indeterminate bridge, the maximum tensile stresses calculated were in the range of 1.65 and 1.85 MPa (240 and 265 psi). For the Utah Bridge, which behaves as a statically determine bridge, the maximum tensile stresses calculated were in the range of 5.8 and 4.5 MPa (850 and 660 psi) These tensile stresses represented a significant percentage of the allowable or direct tensile stress of a structure as per AASHTO LRFD Specifications (2010), therefore significant for design.

Thermal Stresses and Cracking of Concrete Bridges (Elbadry and Ghali, 1986)

Temperature variations acting on a bridge structures depend on geometry, location and orientation, bridge properties and conditions and weather conditions. A nonlinear temperature distribution through the bridge cross section is caused by the relatively low thermal conductivity of the concrete and variation with time of most of the previous conditions. This nonlinear temperature distribution produces stresses in the transverse and longitudinal directions.

In statically determine bridges, nonlinear temperature distribution produces stresses in the longitudinal direction that are self-equilibrating (their resultants are equal to zero) and no variations in reactions occur. In statically indeterminate bridges, the curvature due to temperature will be restrained and statically indeterminate reactions and continuity moments will develop. Therefore, the resulting stresses (also referred as continuity stresses) are produced thus added to the self-equilibrating stresses to obtain the total thermal stresses. As a result of this temperature variations, tensile stresses can be induced in both statically determinate and indeterminate bridges and for pre-stressed concrete bridges, a more detailed design would be required.

For his investigation, Elbadry and Ghali considered a three (3) span continuous bridge in Calgary, Canada with the following dimensions: overall length: 116 m (380 ft), with a main span: 58 m (190 ft). The cross section was made up of one cell box 2.74 m (9 ft) deep. This bridge was partially pre-stressed, some limited tensile stresses were allowed under the effects of gravity loads, while cracking was only allowed under the combination of gravity and temperature loads.

The predicted sum of self-equilibrating and continuity stresses (also called total thermal stresses) indicated a tensile stress of 2.76 MPa (400 psi) occurring near the bottom fiber over the entire length of the span. Also it showed that the stresses due to temperature were of the same order of magnitude as the stresses due to service loads. Therefore, when the stresses due to temperature and service loads were combined, tensile stresses at the bottom fibers exceeded the strength of concrete (f_r) and cracking occurred. Thus, it can be concluded that bridges may be

designed to have no cracks under service gravity loads, but cracking due to temperature variations is most likely to occur. To maintain serviceability, cracks should be controlled by providing a feasible amount of non-pre-stressed reinforcement.

Design of Concrete Bridges for Temperature Gradients (Priestley, 1978)

The design for temperature variations in concrete bridges has traditionally been neglected as a simple matter. Maximum temperature changes induce longitudinal movements, often accommodated by providing sliding joints, bearing displacements or a flexible pier design. In New Zealand, severe cracking of Auckland's new market viaduct, a major urban pre-stressed concrete box girder bridge, stimulated a research conducted by M. J. Nigel Priestley on temperature distribution. A strong correlation was found between the cracks width, ambient temperature and solar radiation. Also transverse variation in temperature through the thickness of webs in box girder bridges was identified as a factor contributing overstress, but it was not considered as a major issue since the primary problem was associated with vertical temperature gradients induced by solar radiation and ambient temperature variation. After the results, Priestly separated the design problem into three major phases.

First, predicting the critical design gradient based on known local ambient characteristics. Since, thermal variation in the longitudinal axis of the bridge was not significant, a two dimensional finite-element of the bridge section analyzed. As

mentioned before, transverse heat flow is insignificant, and a one dimensional finite differential equation was developed for temperature analysis.

Second, calculating stress levels induced in the bridge superstructure by the design thermal gradient. Stresses were calculated by simple statics. However, since the temperature variation is nonlinear and the Navier-Bernoulli hypothesis states that plane sections remain plane is applied, an internal force is created to maintain the final linear strain profile. During the investigation, it was noticed that longitudinal flexural stresses induced by restraint of vertical temperature gradients were the most significant effect of thermal loading since they increased shear force in the end spans therefore increasing the possibility of bearing failure occurring at the abutments. The design thermal gradient for continuous bridges was defined as the one likely to occur within the expected life of the bridge and that could induce maximum tension stresses with consequent serviceability problems since thus cracking may occur. Priestley's investigation indicated that a standard design thermal gradient could be synthesized as a fifth power temperature decrease from a maximum T at the top of the concrete deck to a zero at a depth of 1200 mm (47.2 in.) and a linear increase in temperature over the bottom 200 mm (7.9 in.) of the section. For superstructures with depths less than 1400 mm (55.1 in.) the two components are superimposed.

Third, influence of the thermally induced stresses to serviceability and ultimate load states. Priestley concluded that in normal reinforced concrete bridges, substantial cracking occurred under dead load plus live load, prior thermal loading. The reduced flexural rigidity resulted in reductions in thermal continuity moments.

For pre-stressed concrete, a feasible design approach would be to ignore thermal loading and rely on the reduction in flexural rigidity on cracking to alleviate thermal effects, as with reinforced concrete. He recommended using additional mild steel or a lowered cable profile to reduce crack widths. At service loads, the total effect is found by adding the thermal deformation T to the deformation induced by dead plus live loads. At ultimate load, priestly used the same approach as before, but with the factored thermal deformation is added to the deformation induced by the factored service loads. This type of approach is more significant at service loads than at ultimate loads, due to the nonlinearity of the force deformation curve at ultimate loads.

Proposed Design Method for Thermal Bridge Movements (Roeder, 2003)

The temperatures used for thermal design movements in the AASHTO Specifications (i.e. 1996, 1998) sometimes predicted movements that were larger or smaller that needed. Since bridges expand and contract due to temperatures changes, bearings and expansions joints are usually used to accommodate movements. Bearings and joints are depended upon the design movements and more maintenance over its life time.

Roeder presented a new method for determining bridge design temperatures and thermal movements. According to his investigation, bridge movements are controlled by the average temperature of its cross section. T_{avg} is a weighted average of the bridge temperature over the bridge cross section based upon equilibrium. Minimum values of T_{avg} occur in the early morning hours of the coldest winter

nights, and maximum T_{avg} values occur in mid-afternoon of the hottest summer days.

$$T_{avg} = \frac{\sum A_i * E_i * \alpha_i * T_i}{\sum A_i * E_i * \alpha_i} \quad (1)$$

A method implemented by Kuppa was used to calculate $T_{avg\text{-}max}$ and $T_{avg\text{-}min}$. For the development of this method, Kuppa calculated bridge temperatures (including conduction, convection, and radiation heat flow), geometry and properties along with actual air temperatures, cloud cover, precipitation and wind velocity for a range of different bridges and sites. Local temperatures distributions were used to determine T_{avg}, but the calculations focused on extreme weather conditions ($T_{avg\text{-}max}$ *and* $T_{avg\text{-}min}$) rather than intermediate conditions. This work showed that $T_{avg\text{-}max}$ can be correlated to the average high air temperatures over four consecutive days of the very hottest summer weather, and $T_{avg\text{-}min}$ can be correlated to the average of the low air temperature for four consecutive days in the very coldest winter weather. Since the Kuppa method was proven to give more accurate extreme values for $T_{avg\text{-}max}$ and $T_{avg\text{-}min}$ then it was combined with historic weather data compiled by the U.S. Department of Commerce in order to establish extreme $T_{avg\text{-}max}$ and $T_{avg\text{-}min}$ maps for design of steel and concrete bridges. This map showed that bridges can often be designed for smaller movements than required by AASHTO LRFD (1996) provisions. Also, they help eliminate the ambiguity of the cold and mild climate designations in thermal movement design.

Roeder's research with minimal modifications helped build an alternative method for temperature design which has been included in AASHTO LRFD Specifications since 2005.

Prediction of Temperature and Stresses in Highway Bridges by Numerical Procedure using Daily Weather Reports (Thepchatri and Johnson, 1977)

The objective of this study was to develop a method to properly predict bridge temperature distributions and stresses caused by daily environmental changes. Limited types of highway bridges found in Austin, Texas were used for this investigation. The type of bridges studied can be classified as 1) a post-tensioned concrete slab bridge, 2) a composite precast pretension bridge and 3) a composite steel bridge. Thepchatri and Johnson's proposed method was able to solve temperature problems for various types of highway bridge cross sections and different conditions of the environment by using finite-element program which also incorporated heat flow and thermal analysis.

As part of the study, theoretical models based on one and two dimensional heat flow theory along with outgoing radiation (long wave) were used to predict the nonlinear temperature distribution over the bridge cross section (horizontally and vertically). For the analysis, past records of solar radiation levels and daily air temperature distribution were used. Similarity in the resulted predicted and measured data validated the numerical method proposed. It was noted that even though this study was focused for structures located in Austin, Texas, other structures can be analyzed by adjusting important weather parameters (radiation,

ambient air temperatures and wind speed) to local conditions, along with shape, size and thickness of the structure which all played an important role influencing temperature variations.

Thermal deflections were found to be small not being the same for the longitudinal movement which exceeded the value suggested by ASSHTO'73 Specifications. It was also found that the interface shear force caused by the temperature difference between the slab and the beam was of such a magnitude that a slip effect could be caused.

CHAPTER 3

THERMAL ANALYSIS

Bridge Description

California Bridge

The California Bridge that was used for this study is located near Elk Grove, California which is approximately 30 miles south of Sacramento. It is part of the Interstate-5 (I-5) corridor crossing over Lambert Road, a very lightly traveled country road. The bridge currently accommodates two southbound lanes of traffic with an Average Daily Traffic (ADT) of approximately 24,500 vehicles and an Average Daily Truck Traffic (ADTT) of 23%. The construction of the bridge was completed in 1975. Figure 20 located in Appendix 1 show aerial views of the bridge. The superstructure of the bridge was designed as a cast-in-place, post tensioned, box-girder bridge. The bridge superstructure is supported with a center reinforced concrete pier and reinforced concrete integral abutments at each end. The California Bridge has an overall span length of 78.6 m (257.9 ft) with an 8˚ skew. The overall length is comprised of two equal spans of 39.3 m (129 ft). The spans were designed as live-load continuous. Figure 1 shows a plan view of the California Bridge.

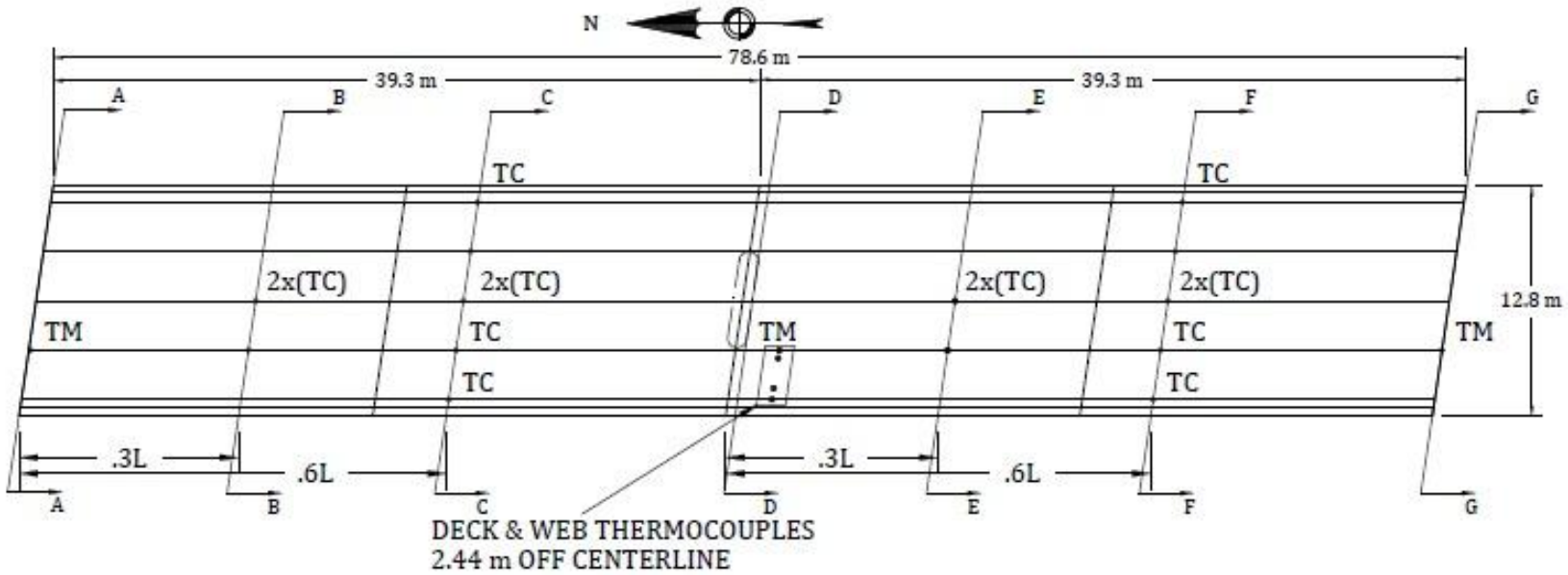

Figure 1 - Plan view of the California Bridge with Thermocouples and Tilt-meters located.

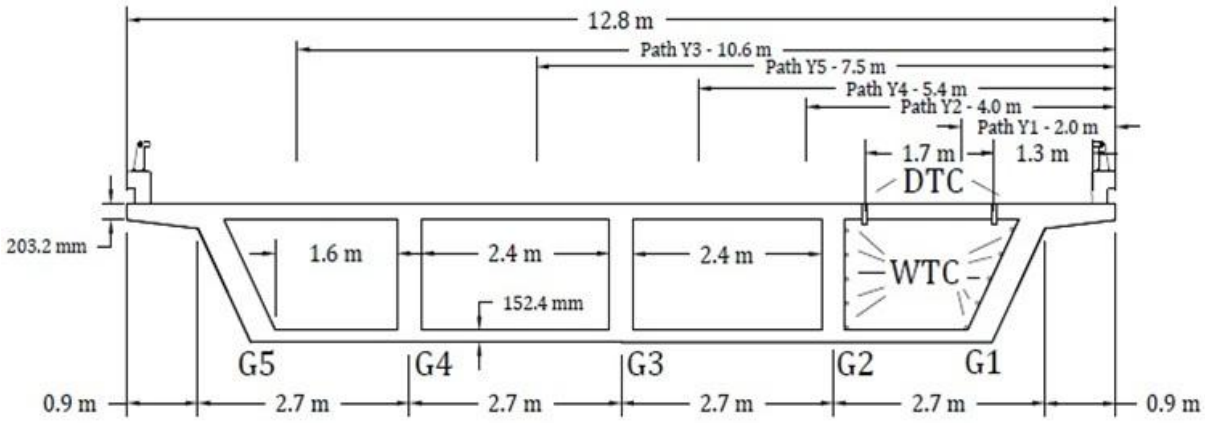

Figure 2 – Cross Section View of the California Bridge.

The total width of the bridge deck is 12.8 m (42 ft) with an actual road width of 12.2 m (40 ft). Concrete barrier railings 328 mm (12.0 in.) wide and 806.4 mm (32.0 in.) height are located on each side along the entire length of the bridge. The box girder depth is 1.7 m (66.0 in.) including the deck. It is composed of four cells (5 webs) with an interior spacing of 2.7 m (9.0 ft). The exterior webs have a slope of 2:1 and an overall average thickness of 300 mm (12.0 in.).

The average thickness of the reinforced concrete deck is 203.2 mm (8.0 in.) with an overhang distance measured from the centerline of the exterior girders of 0.9 m (3.0 ft). The average thickness of the bottom flange is 152.4 mm (6.0 in.). Figure 2 shows a cross sectional view of the bridge.

The concrete used in the superstructure had a specified compressive strength (f'_c) at releasing of the post-tension strand of 24.2 MPa (3,500 psi). Grade 60 (GR60) mild reinforcing steel was used in all elements of the structure except in the deck and diaphragms where Grade 50 (GR50) steel was used.

The five web girders were post-tensioned with low relaxation, grouted post-tensioning strands, with a specified yield and ultimate strength of 1.65 GPa and 1.86 GPa (240.0 ksi and 270.0 ksi), respectively. The strands followed a parabolic shape throughout each span. The post-tensioned strands in each girder were jacked to a total force of 7,520 kN (1,690 kips). The strand centroid is located at 890 mm (35.0 in.) from the bottom of the bottom flange at the end abutments and 1,295 mm (51.0 in.) from the bottom at the pier support. At its lowest point, located at 3.9 m (12.9 ft) from the mid-span of each span, the centroid of the strand is located at 279 mm (11.0 in.) from the bottom of the bottom flange.

The bridge is supported at the mid-span by a column with a bent cap of the same width of the bridge and with a thickness of 1.83 m (6.0 ft). The column is 1.07m (3.5 ft) thick with a bottom width of 3.66 m (12.0 ft) increasing with its height (14:1 slope). It is supported by a foundation cap of 5.48 m x 3.66 m x 1.07 m (18 ft x 12 ft x 3.5 ft) on twenty four Φ 406.4 mm (16.0 in.) diameter drilled concrete piles with a capacity of 623 kN (70 tons).

The integral abutments are 0.76 m thick x 3.05 m deep (2.5 ft x 10.0 ft) supported by a reinforced concrete pile cap of 12.96 m x 1.22 m x 0.46 m (4.25 ft x 4.0 ft x 1.5 ft). Each pile cap transfer the load to seven Φ 406.4 mm (16.0 in.) diameter drilled concrete piles with a capacity of 623 KN (70 tons).

Utah Bridge

The Utah Bridge is located near West Perry, Utah which is approximately 60 miles north of Salt Lake City. It is part of the Interstate-15 (I-15) corridor crossing

over Cannery Road a very lightly traveled road. The bridge consists of two northbound lanes of traffic carrying an Average Daily Traffic (ADT) of approximately 22,200 vehicles a day with an Average Daily Truck Traffic (ADTT) of 29%. Construction was completed in 1976. Figure 21-Figure 22 located in Appendix 1 show aerial views of the bridge. The superstructure of the bridge was design as a single span, comprised of five pre-stressed I-girders. The bridge had a single mid-span reinforced concrete diaphragm and was supported at both ends with integral abutments. The bridge has an overall span length of 24.9 m (81.7 ft) with a clear span of 24.4 m (80 ft). The total width of the deck is 13.4 m (44 ft) with an actual road width of 12.4 m (40.5 ft). Figure 3 shows a plan view of the Utah Bridge.

The concrete used in the superstructure had a specified compressive strength (f'_c) of 27.6 MPa (4,000 psi). Grade 60 (GR60) mild reinforcing steel was used throughout structure. The superstructure is composed of five pre-stressed concrete AASHTO Type IV girders, with a length of 25.2 m (82.5 ft). These girders were spaced at 2.7 m (8 ft-10 in.) on center. The five precast concrete girders were pre-stressed with a harped tendon profile. At the girder ends, the centroid of the pre-stressing strands is located at 340.2 mm (13.5 in.) from the bottom of the girder. The harping point is located 9.75 m (32.0 ft) from the ends of the girder and the centroid of the pre-stressing strands is located at 102.8 mm (4.1 in.) from the bottom of the girder. The final pre-stressing force after all losses was estimated to be 3,367.3 kN (757 kips).

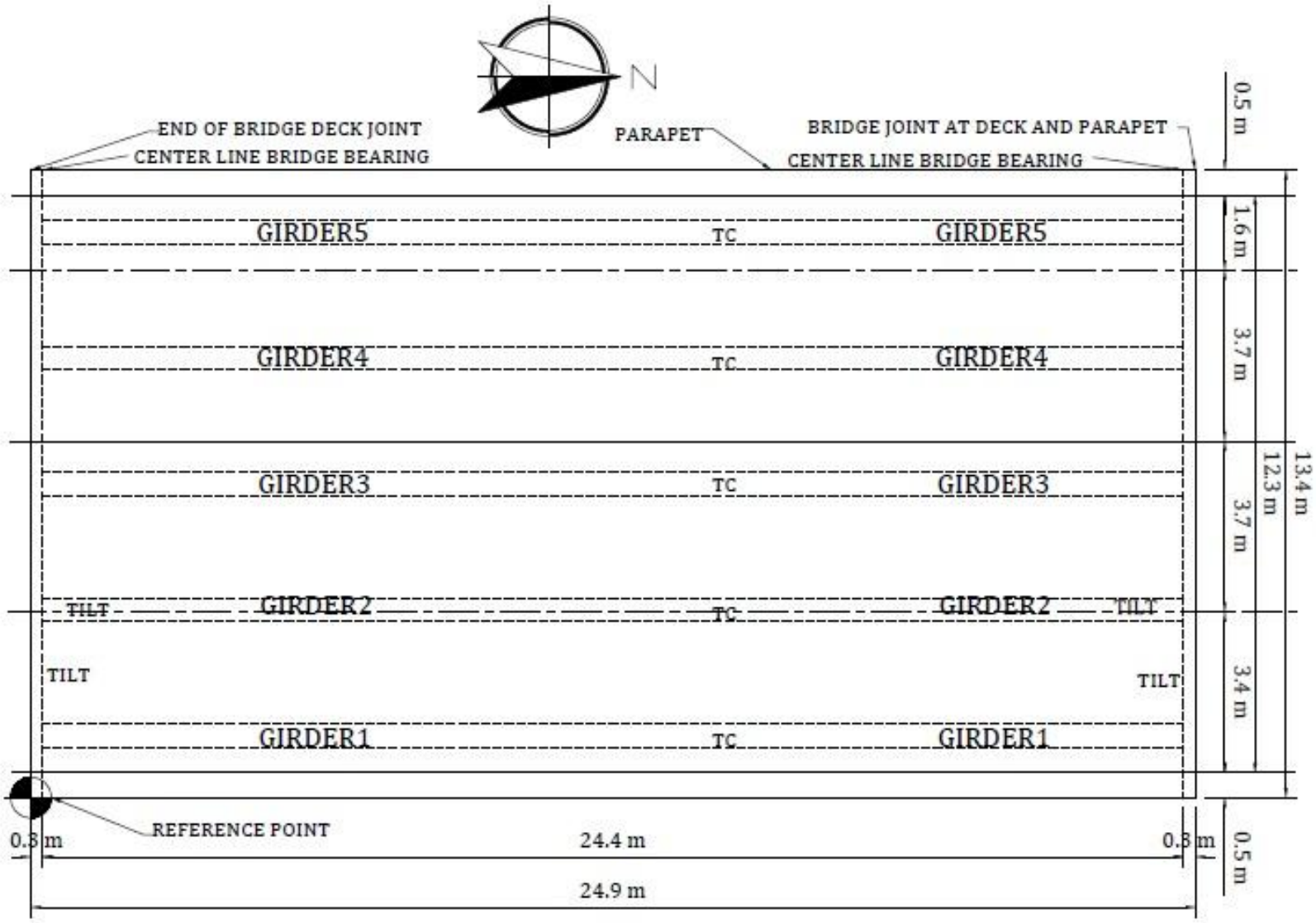

Figure 3 – Plan view of the Utah Bridge with Thermocouples and Tilt-meters located.

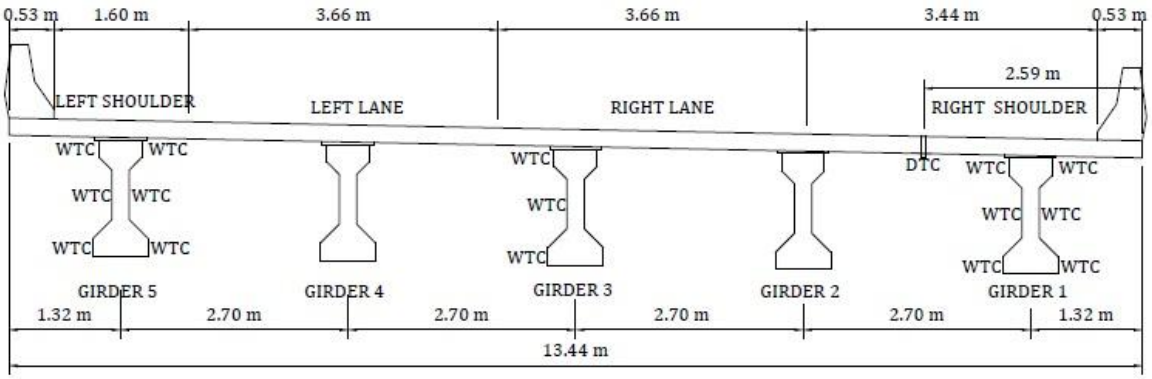

Figure 4 – Cross Section View of the Utah Bridge.

Concrete barriers that are 530 mm (20.9 in.) wide and 1,070 mm (42 in.) in height are located all along each side of the bridge. The average deck thickness of the deck is 200 mm (8.0 in.) with an additional specified 76.2 mm (3 in.) thick asphalt membrane. Figure 4 shows a cross sectional view of the Utah Bridge.

The Utah Bridge is supported with integral abutments that are of 0.76 m thick x 3.20 m deep (2.5 ft x 10.5 ft) transferring the load to five Φ 762 mm (30.0 in.) reinforced concrete drilled piles with a total maximum allowable of 1,780 kN (400 kips).

Bridge Instrumentation

Descriptions

In order to quantify the overall bridge response due to temperature effects, a comprehensive instrumentation plan was prepared to provide continuous evaluation and structural health monitoring of both the California and Utah bridges. Many factors that affect bridge performance due to seasonal and daily temperature

variations were considered when developing this instrumentation plan. To capture overall system behavior during seasonal thermal variations, two different types of sensors were installed on both bridge structures: tilt-meters and thermocouples.

Thermocouples were strategically installed over the height of the bridge superstructure with the intention of measuring temperature gradients as well as providing enough resolution to obtain uniform temperature differentials. The changes in temperature measurements throughout the depth of the cross section allowed researchers to understand diurnal and seasonal effects on the structures such bridge deflections. The tilt meters measure the static rotation at the abutment of the girders due to thermal changes.

In order to provide information based on environmental conditions and climate, a weather station tower with various measurement devices was installed at the Utah Bridge site. The measurements devices included wind speed, wind direction, ambient temperature, relative humidity, solar radiation and rain detection. Ambient temperature data was recorded in order to correlate its variation with the temperature gradients and average bridge temperature in a given day.

California Bridge Instrumentation

The effect of changes in temperature on the California Bridge was monitored using a total of forty-seven sensors. In order to obtain measurements of the concrete temperatures occurring at various locations along each span and deck of the bridge, a total of forty-four thermocouples were installed. Fourteen thermocouples were

placed at the bottom of the web of girders, seven thermocouples equally distributed on each span and located at 11.8 m and 23.6 m of the center pier (38.7 ft and 77.4 ft) as shown by sections CC and FF in Figure 1. Ten thermocouples were installed on an exterior and interior web girder (G2 and G1), inside the cell box of the south-span of the bridge and located at 2.44 m (8.0 ft) from the center pier as shown in Figure 2. To record temperature changes throughout the height of the concrete deck, two groups of ten thermocouples were installed aligned longitudinally with the web thermocouples starting at 6.35 mm (0.25 in.) from the top of the deck and ending at 190.5 mm (7.5 in.). Figure 23-Figure 24 located in Appendix 2 show how the thermocouples are installed.

Three tilt meters were also installed on the bridge superstructure in order to measure changes in rotations of the supports of the girders due to various thermal loading conditions. One tilt meter was installed at each abutment and one additional tilt-meter was attached at the central pier as shown in Figure 1.

Utah Bridge Instrumentation

For the Utah Bridge, thirty-four sensors were used to quantify its thermal behavior. A total of 34 thermocouples were installed in order to obtain readings of the concrete temperatures occurring along the bridge superstructure. Five thermocouples were placed at the bottom of the web of girders, located near mid-span at 12.4 m (40.8 ft) of the south abutment as shown in Figure 3. An additional fifteen thermocouples were installed on the web of the two exterior (inside and outside face) and one interior center girders located at 15.5 m (50.8 ft) of the south

abutment as shown in Figure 3. These web thermocouples were installed at 101.6, 685.8 and at 1,117.6 mm (4 in. , 27 in., and 44 in.) from the bottom web as shown in Figure 4. In order to measure the temperature changes throughout the depth of the concrete deck, a group of ten thermocouples were installed, which are also aligned longitudinally with the web thermocouples, starting at 6.35 mm (0.25 in.) from the top of the deck and ending at 190.5 mm (7.5 in.). Figure 25 Figure 26 located in Appendix 2 show how the thermocouples are installed.

Four tilt-meters were installed at various locations of the bridge. One tilt-meter was attached to the abutment at each end of the bridge to measure the rotation of the abutment to girders. The other two tilt-meters were attached at each end of Girder 2 to measure the rotation of the girder itself as shown in Figure 3.

All instruments were connected to AM25T twenty-five-Channel Solid State Multiplexer and a CR1000 Campbell Scientific data logger with internet capabilities, installed at the respective bridge sites. The data logger was programmed to collect and record raw data every 15 minutes. All measurements were downloaded to a computer at Utah State University via a remote communication connection, in the form of high-speed internet service.

Measured Average Temperature

Bridge temperatures have been found to vary over the bridge cross section as a function of time. Temperature measurements acquired with bridge instrumentation installed on the California and Utah Bridges were used to obtain daily maximum and minimum average temperature variations. According to the current version of the AASHTO LRFD Bridge Design Specifications (2010), the average temperature (T_{avg}) is a weighted average of the bridge temperature over the bridge cross section based upon equilibrium as shown in Equation 1. This relationship is based on previous research done by Roeder (2003).

$$T_{avg} = \frac{\sum A_i * E_i * \alpha_i * T_i}{\sum A_i * E_i * \alpha_i} \quad (1)$$

where

T_{avg} = average of the bridge temperature over the bridge cross section;

A_i = Area of the bridge cross section of the *i*-th segment;

E_i= Modulus of elasticity of the cross section of the *i*-th segment;

α_i= Coefficient of thermal expansion of the material used for the *i*-th segment;

T_i= Temperature of the cross section of the *i*-th segment.

Equation 1 was used to calculate the average bridge temperature at the 15 minute recording intervals. The time of minimum values (T_{avg}) for both bridges occurred in the early morning hours of the coldest winter nights, and maximum values of T_{avg} occurred in mid-afternoon of the hottest summer days. These

calculated mean temperatures were compared to the temperature ranges specified in the AASHTO LRFD Bridge Design Specifications (2010). Currently, the AASHTO Specifications recommends two procedures to determine the range of mean temperature. Procedure A classifies the zone where the structure is located as a Cold or Moderate climate, depending on the total amount of freezing days in a year. Procedure B is based on previous research (Roeder 2003) and it provides contour maps with extreme bridge design temperature registered over a period of 60 years. Both procedures were compared for this study.

For the California Bridge, the AASHTO LRFD Bridge Design Specifications (2010) recommends a temperature range of 46 ˚C (115 ˚F) to -1 ˚C (30 ˚F) for the maximum and minimum mean bridge temperature range, respectively. During this study, the maximum and minimum mean temperatures per month obtained from the California Bridge were 43.0 ˚C (109.5 ˚F) and 3.5 ˚C (38.2 ˚F) as shown in Figure 5. For the Utah Bridge, the AASHTO LRFD Specifications (2010) recommends a temperature range of 46 ˚C (115 ˚F) and -23 ˚C (10 ˚F) for the maximum and minimum bridge temperature, respectively.

During this study, the maximum and minimum mean temperatures per month obtained from the Utah Bridge were 34.1 ˚C (93.3 ˚F) and -12.8 ˚C (8.9 ˚F) as shown in Figure 6. For the Utah Bridge, the maximum averages value was not as close to the maximum AASHTO value as with the California Bridge in part believed to the asphalt overlay on the Utah Bridge and the temperature readings starting in September. Despite the limited data, the range in measured temperature variations show that the mean temperature vary significantly over the course of the year.

Comparison between the maximum and minimum average temperatures recorded in a month with the extreme limits provided by the design maps is also shown in Figure 5 and Figure 6. The calculated mean temperatures are well within the range defined by the extreme limits provided by the design maps but clearly approaching the design limits during summer and winter extremes, in some cases with only a slight difference of 3 ˚C (6.5 ˚F).

In addition to the deck thermocouples installed on the Utah Bridge, a weather station was also installed by the researchers adjacent to the bridge, as shown in Figure 27 located in Appendix 2. This weather station recorded the ambient temperature at the same time the various concrete temperature were measured.

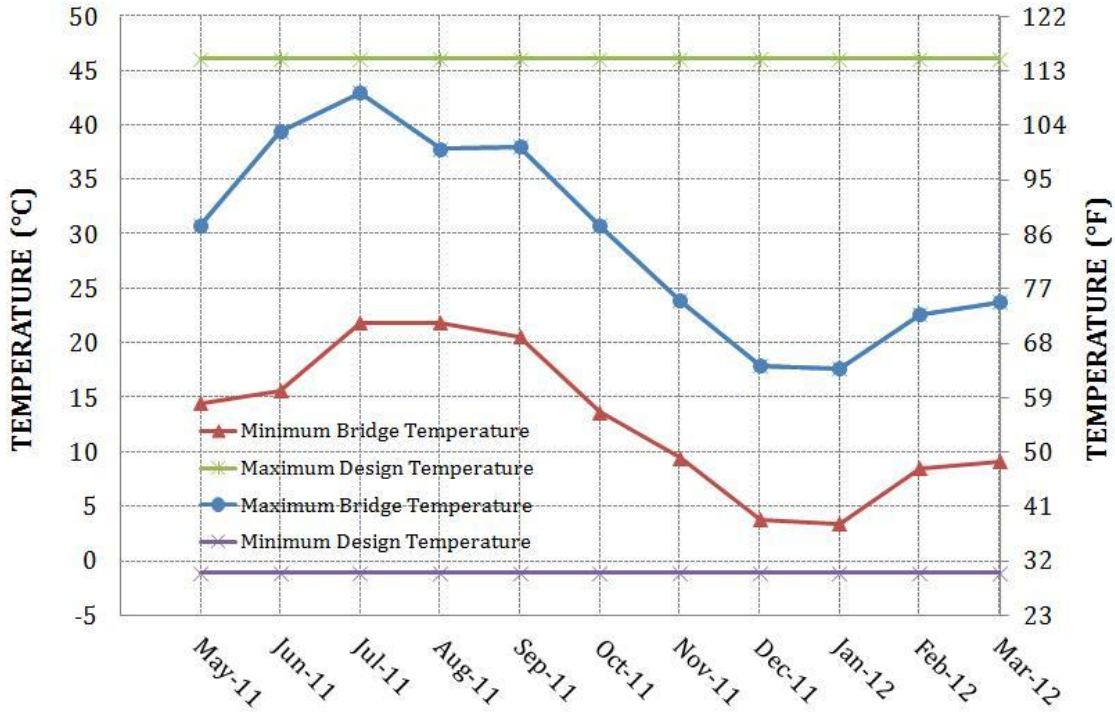

Figure 5 – Monthly measured mean temperature for the California Bridge.

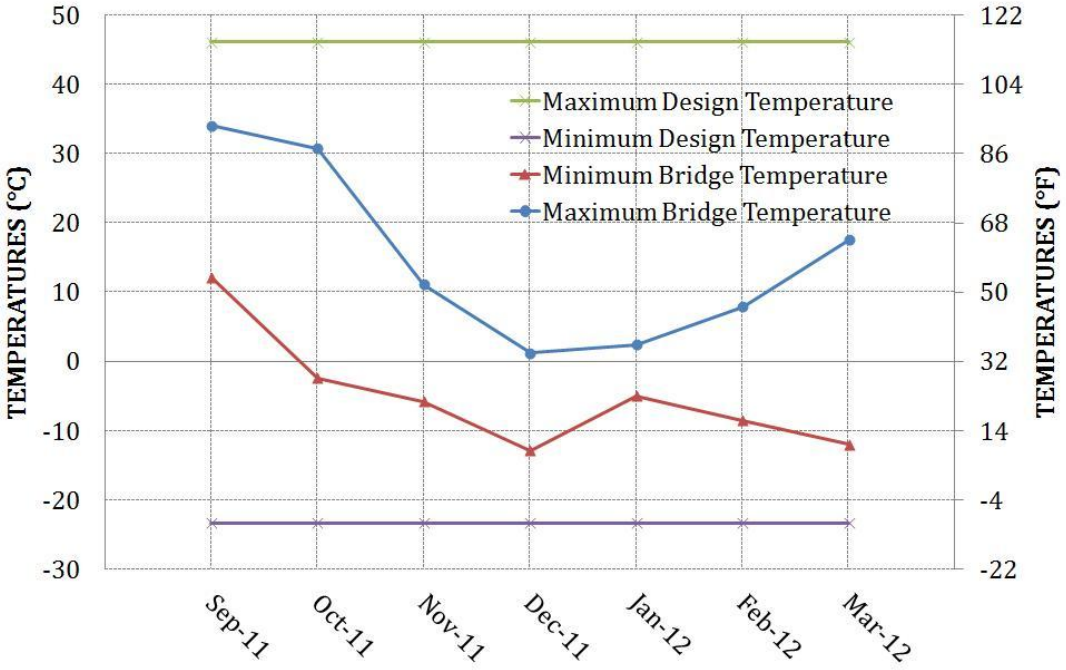

Figure 6 – Monthly measured mean temperature for the Utah Bridge.

Figure 7 shows a correlation between daily calculated mean temperatures and measured ambient temperature at the station weather. The maximum ambient peak temperature is on average 2.1 ˚C (3.8 ˚F) larger than the maximum mean bridge temperature. In general, the minimum ambient temperature is closer to the mean bridge temperature.

Figure 8 shows a how the maximum and minimum average bridge temperatures are correlated to the maximum and minimum temperatures of over a several week period. This figure indicates that the maximum and minimum average bridge temperatures are related, at least for the Utah Bridge, to the ambient temperature throughout the day. A best fit equation was obtained and showed that the relationship was linear with a coefficient of correlation of 0.93.

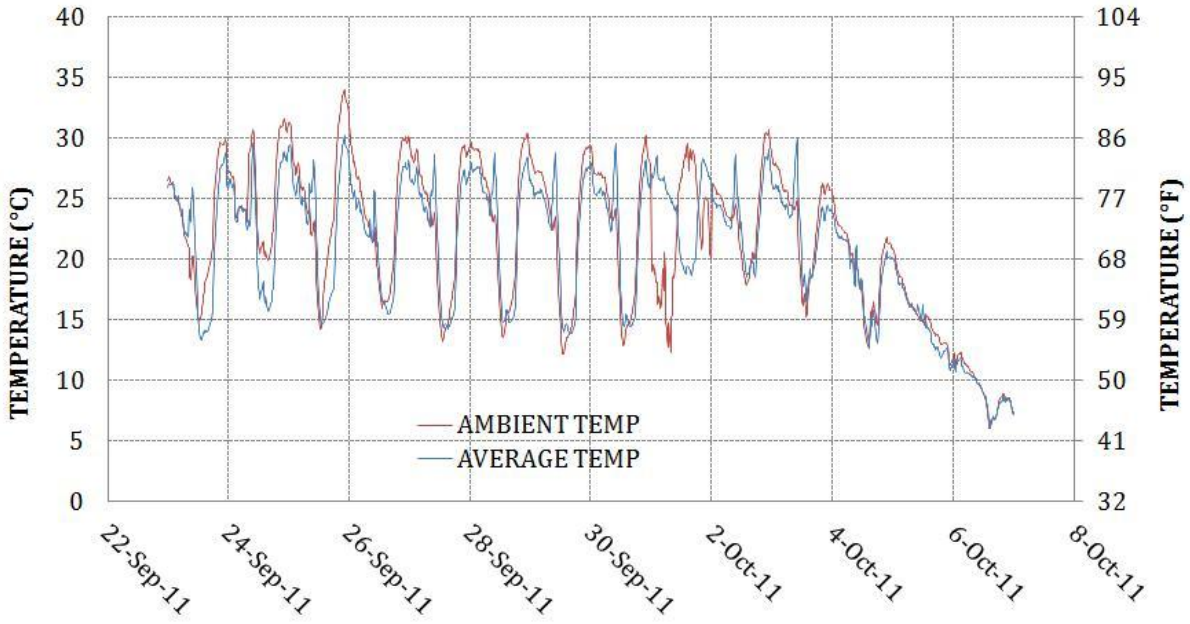

Figure 7 – Monthly measured mean temperature on the Utah Bridge.

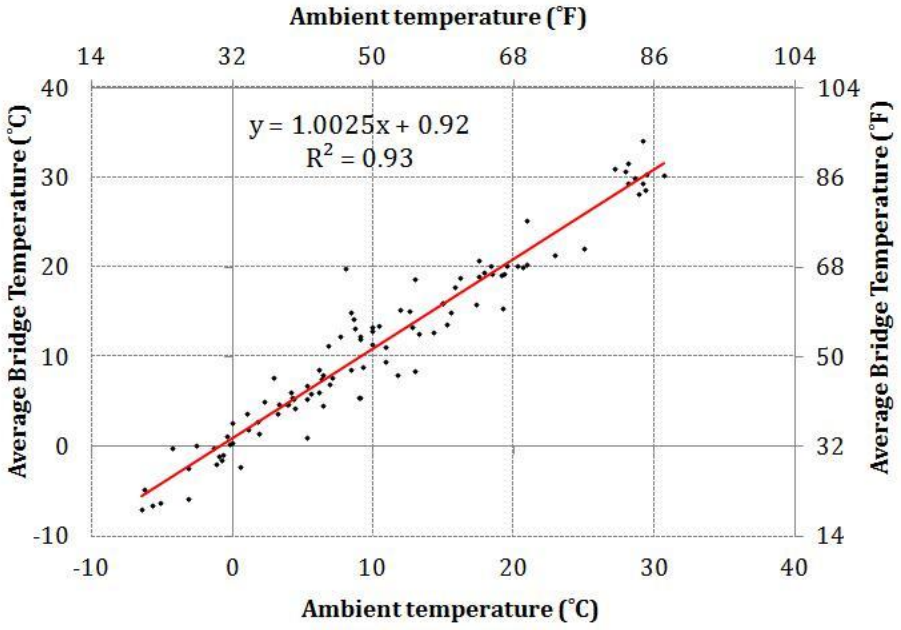

Figure 8 – Comparison between Average Bridge Temperature and Ambient Bridge Temperature.

Using this proposed relationship, a comparison between methods from previous researches (i.e. Moorty and Roeder 1992; Emerson 1982) was made. The Emerson method provided better estimates of the day-to-day bridge temperature, but the Kuppa method provided more accurate estimates of extreme $T_{avg\text{-}max}$ and $T_{avg\text{-}min}$ (Roeder 2002). A linear correlation was used using average conditions, since small amount of extreme data is available. These models produced temperature predictions very similar to our measured data, being the temperatures range predicted by Kuppa's method closer to it, as shown in Figure 9.

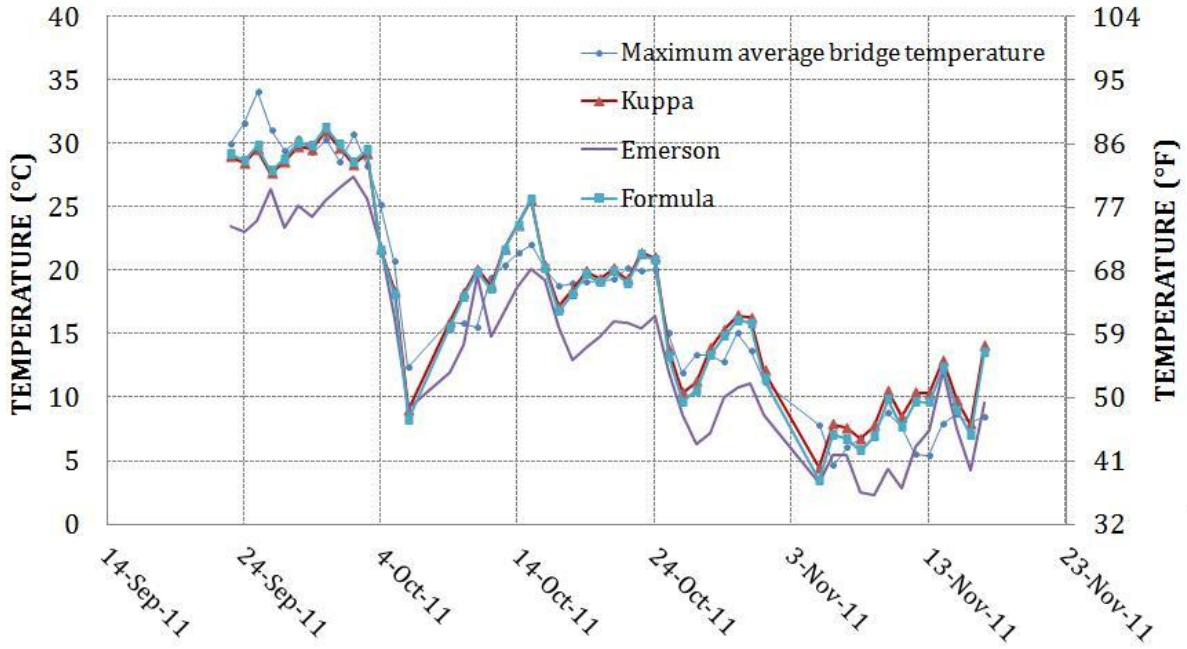

Figure 9 – Comparison between measured temperatures and other researches.

Measured Temperature Gradients

The current AASHTO LRFD Bridge Design Specifications divides the United States into four climate zones and assigns different thermal gradients for bridge superstructures located in each of these regions. According to previous editions of the AASHTO Specifications (i.e. AASHTO LRFD Specifications 1994) and other researchers (i.e. Priestley 1978; Imbsen 1985), the presence of an asphalt overlay and other possible thermal isolation was taken into account in determination of the design gradients. However, the current AASHTO LRFD Specifications (2010) obviate this thermal isolation effect, and for the design thermal gradient does not take into account the presence of an asphalt overlay on top of the concrete deck.

In addition, even though the temperature gradient is included in various load combinations, the AASHTO LRFD Specifications (2010) specifies that it can be neglected if experience has shown that temperature effects are not an issue. Previous researches have shown damage or failure of bridge superstructures due to thermal effect or inaccurate thermal analysis, which may lead to serviceability problems if not properly taken into account.

Throughout the year the magnitude of the temperature gradient varies with ambient conditions. To better understand the changes in the thermal gradient for the two instrumented bridges, measured temperatures from the thermocouples installed over the height of the cross-section of the bridges were evaluated. Since an extremely large amount of measurement readings were recorded at the 15 minute reading interval, a method of organizing and classifying the data was utilized. The

data was classified using: 1) a day-by-day basis; and 2) a month-by-month basis (critical days only).

Maximum Positive and Negative Gradient Determination

Because the bridge temperature gradient is defined as the difference in concrete temperatures over the height of the structure, the largest recorded difference over the defined time period was defined as the maximum temperature gradient. The data was categorized to determine the maximum gradients occurring over the bridge cross section through the course of the monitored months. From the measured data, it was observed that, in general, the most uniform region of temperature measurements occurred throughout the girder web which allowed using it as a base line to calculate the top and bottom gradients for each measurement time. This uniform region helped identify the largest positive and negative temperature gradients corresponding to the daily temperature changes for each month. Based on the data, it was determined that the largest positive gradients temperatures typically occurred during mid-afternoon and largest negative gradients typically occurred in the bridge during the early morning hours of each day.

For the California Bridge, the largest positive gradient of 24 ˚C (53 ˚F) was observed at 3:00 pm on July 2. This maximum positive gradient is plotted in Figure 10 and it is compared with the positive design gradient presented in the current and previous versions of the AASHTO LRFD Code, along with the thermal gradient recommended by Priestley (1978). The maximum measured temperature at the top

of the deck was smaller than the predicted values but represents a typical California summer. Presumably with more data, the difference would be minimized. The shape of the measured temperature gradient more closely resembled the AASHTO LRFD distribution in comparison to the Priestley distribution in that the concrete temperature became uniform closer to the top flange. At the bottom flange, both the AASHTO LRFD and Priestley distribution methods predicted the temperature gradient reasonably well.

Similarly, the maximum negative gradient of -8.0 ˚C (-14.4 ˚F) was observed at 5:45 am on June 24 (Figure 11). The figure also shows the recommended negative design gradient presented in the 1994 and 2010 versions of the AASHTO LRFD Specifications, and the negative thermal gradient proposed by Priestley (1978). It is interested to note that the top negative thermal gradient is perfectly encompassed by the AASHTO LRFD codes and Priestley's gradients, but the bottom gradient measured -7.8˚C (-14.2 ˚F) is three times as much as all the design gradients. This larger bottom temperature gradient was consistent throughout the recording period.

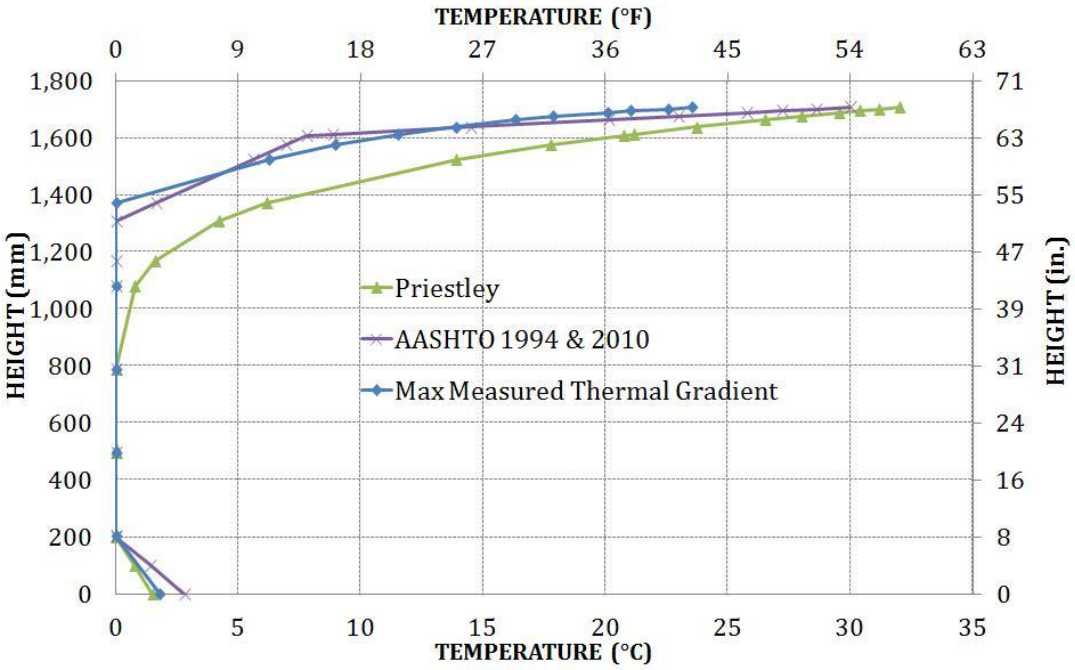

Figure 10 – Maximum positive thermal gradient for the California Bridge on July 2.

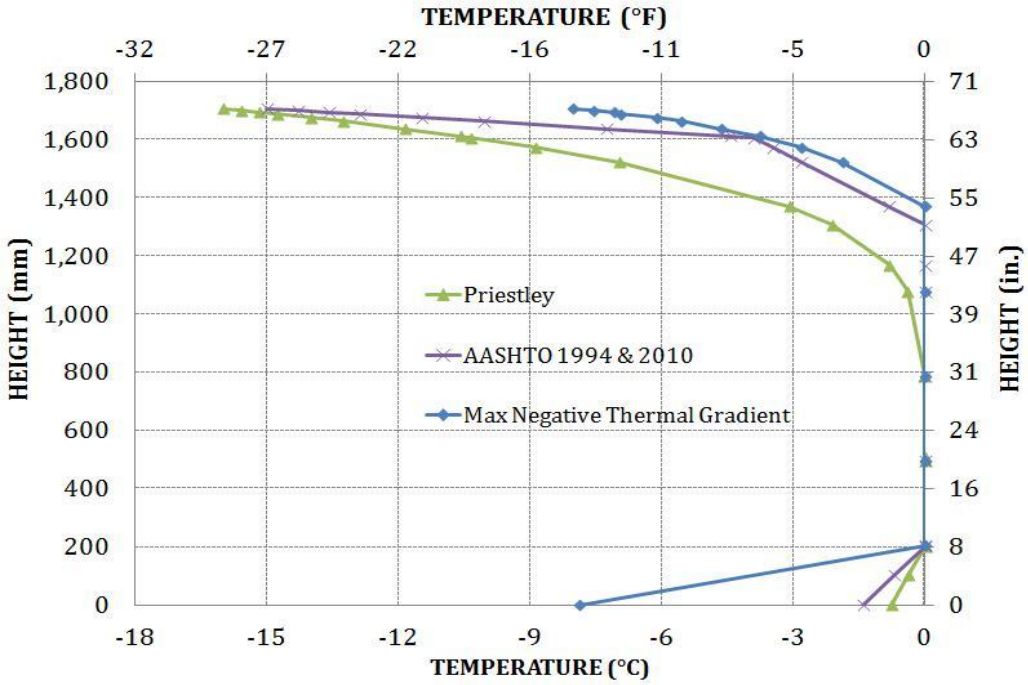

Figure 11 - Maximum negative thermal gradient for the California Bridge on June 24.

For the Utah Bridge, the highest top positive gradient of 17 ˚C (31 ˚F) was observed at 1:45 pm on September 25 (Figure 12). This maximum positive gradient is also compared with the design gradient presented in the current and previous versions of the AASHTO LFRD Specifications, and the thermal gradient proposed by Priestley (1978). The gradients plotted from the AASHTO LRFD 1994 Specifications and Priestley's investigations include the effect of an assumed thermal isolation provided by the asphalt overlay. It is interested to note that the top thermal gradient is almost identical to that of the AASHTO LRFD 1994 Specifications, but Priestley's gradient underestimates its values and the current AASHTO LRFD provisions (2010) overestimates the gradient. This would indicate that the effect of the asphalt overlay may be significant. Also notice that the bottom gradient measured 9.5˚C (17 ˚F) is twice as much as all the design gradients which is similar to the findings of the California Bridge.

Similarly, the maximum negative gradient for the Utah Bridge of -7.10 ˚C (-12.8 ˚F) was observed at 10:00 am on October 9th (Figure 13). The figure also shows the recommended negative design gradient presented in the 1994 and 2010 versions of the AASHTO LRFD Code, and the negative thermal gradient proposed by Priestley (1978). The maximum negative gradient is perfectly encompassed by the AASHTO LRFD codes and Priestley's gradients. The top of the negative thermal gradient is 50% smaller than the design gradients, but the bottom gradient measured -5.8˚C (-10.5 ˚F) is three times as much as all the design gradients.

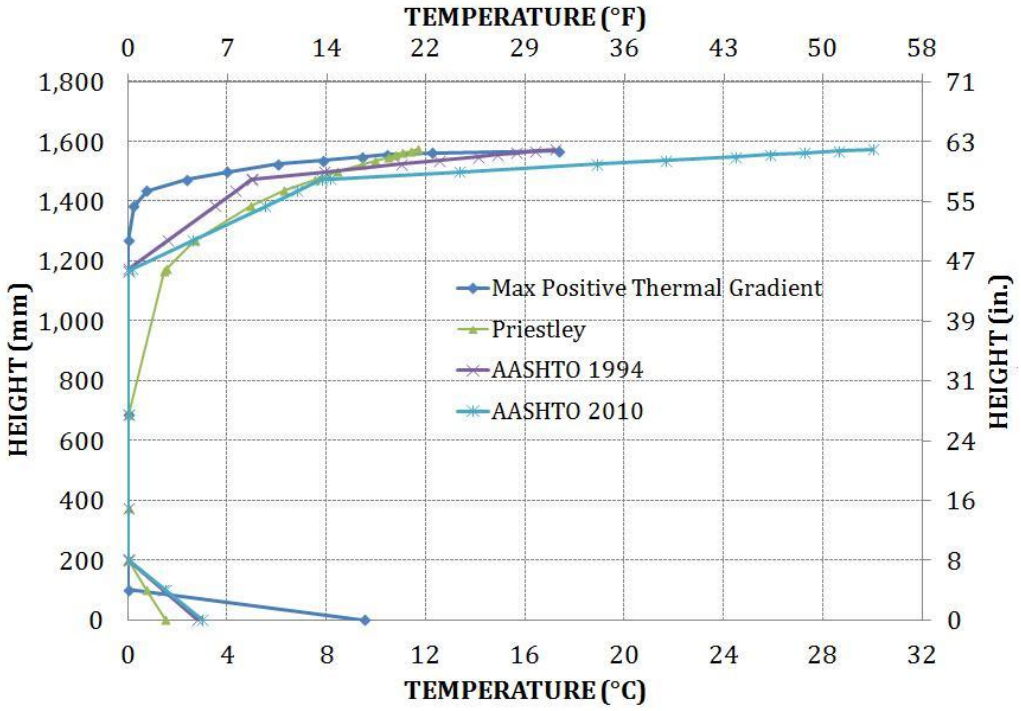

Figure 12 - Maximum positive thermal gradient for the Utah Bridge on September 25.

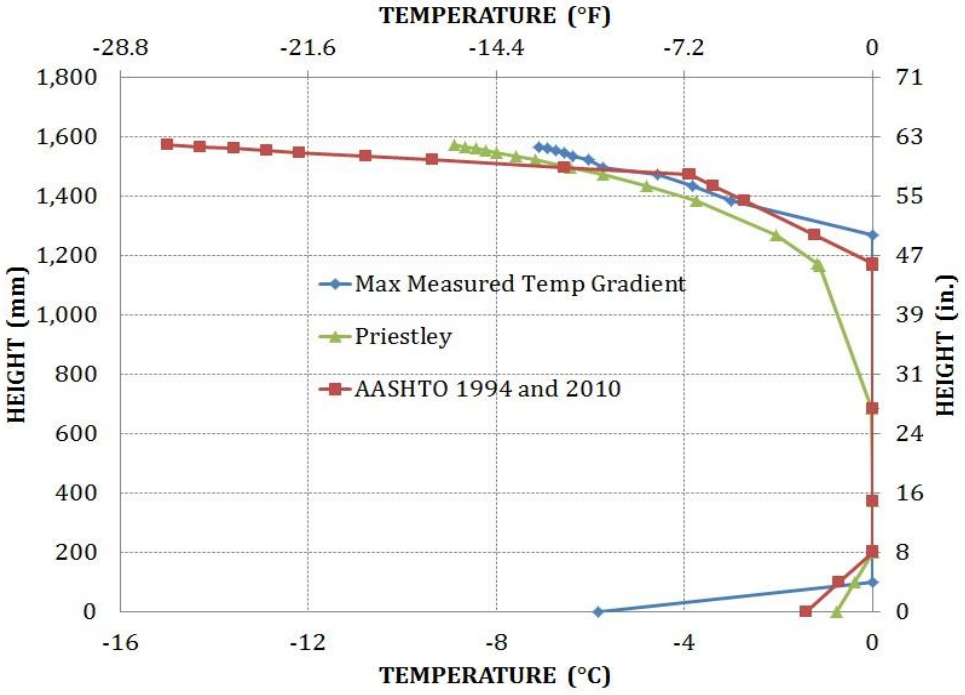

Figure 13 - Maximum negative thermal gradient for the Utah Bridge on October 9.

Finite-Element Model

Finite-element models of the California and Utah Bridges were developed using the finite-element software SAP2000 (Computers and Structures, Inc.). These models were validated using changes in strain from a live-load test in the case of the California Bridge and changes in tilt from the Utah Bridge.

Development and Considerations for the Finite-Element Model (FEM)

Elements Representation and Boundary Conditions

For the California Bridge, the finite-element model was divided into five principal sections: concrete deck, bottom flange, concrete girders, diaphragms and parapets. Each of these bridge sections was modeled using eight node, hexahedral solid elements, except at the diaphragms and skewed end of the bridge where occasionally six nodal triangular solid elements were used due to the bridge geometry. The post-tensioning strands were modeled using tendon elements. Five tendons were used to model the post-tensioning as loads and were discretized in 1.5 m (5 ft) sections along the longitudinal direction. Using the post-tensioning load as a point load where losses (i.e. friction, anchorage, elastic shortening, creep, shrinkage and steel relaxation) were taken into account by applying the effective post-tension force as per the bridge plans.

The concrete deck was modeled using a modulus of elasticity of 24,130 MPa (3,500 ksi) based on the specified deck concrete compressive strength. For girders an average modulus of elasticity of 41,370 MPa (6,000 ksi) was used.

For the Utah Bridge, the finite-element model was developed using eight nodal, hexahedral solid elements for the concrete deck and girders. The concrete deck was modeled using a modulus of elasticity of 27,580 MPa (4,000 ksi). The five precast, pre-stressed girders were modeled using a modulus of elasticity of 41,370 MPa (6,000 ksi). Both the parapets and the mid-span diaphragm were modeled using the same material properties as the concrete deck. The pre-stressing strands were defined in the model using tendon elements forming a harping shape along the centerline of the pre-stressing strands. Using the pre-stressing load as a point load where the pre-stressing losses (i.e. friction, anchorage, elastic shortening, creep, shrinkage and steel relaxation) were taken into account by applying the effective pre-stress force as per the bridge plans.

For both bridges models, the final boundary conditions were adjusted in order to replicate actual bridge conditions and allow the models behavior to coincide with the measured behavior obtained from the field testing. In all cases, the modulus of elasticity was kept near the code calculated value based on the specified concrete compressive strength.

Comparison of Tilt-meter Data vs. Finite-Element Model

It was the original intention to use measured values of end rotation and thermal gradients to validate the finite-element models of both bridges. However due to the very small values of rotation measured on the California Bridge, a live-load test was used to validate that model. The live-load test on the California Bridge was performed to obtain bridge response while being subjected to a truck load driven at approximately 8 km/hr. (5 mph). The results from the live-load test were used to validate the finite-element model. The live-load test consisted of driving two different trucks across the bridge along five selected load paths to maximize the moment in different girders. The load path distances from the centerline of the passenger front axle tire to the edge of the bridge were 2.0 m (6.6 ft) for Path Y1, 4.0 m (13.1 ft) for Path Y2, 5.4 m (17.7 ft) for Path Y4, 7.5 m (24.7 ft) for Path Y5, and 10.6 m (34.8 ft) for Path Y3. An illustration of the transverse axle position on the bridge is shown in Figure 2.

The first truck was a tandem rear axle dump truck with a total weight of 290 kN (65.2 kips). This particular truck had an axle spacing of 5.8 m (19.1 ft) from the front axle to closest rear axle and 1.3 m (4.3 ft) between the back two axles. Each axle weighed 60 kN, 115 kN and 115 kN (13.6, 25.8 and 25.8 kips), respectively. The second truck was a wheel hauler truck with a total weight of 325 kN (73 kips), and a front, middle pair, and a rear pair of axles. The front axle was spaced at 5.3 m (17.3 ft), the middle to back pair spacing was 6.6 m (21.7 ft), with each pair axle spacing being 1.3 m (4.3 ft). Each axle weighted 43.6 kN, 68.5 kN, 68.5 kN, 72 kN and 72 kN (9.8, 15.4, 15.4, 16.2 and 16.2 kips), respectively.

Measured strains were compared with calculated finite-element values in order to determine the accuracy of the finite-element models in predicting the measured response from the live-load test. Using the predicted change in stress due to the application of the live-loads at various locations along the California Bridge and Hooke's Law, the changes in strains caused by bending and axial forces were determined. It was clear that the integral abutment was causing significant restrain at the supports. As per the bridge's boundary conditions measured during the live-load test, the California Bridge behaved in a nearly-fixed end condition. This measured end restraint behavior was modeled by applying spring elements along the top and bottom nodes at both end abutments. The springs were assigned with a constant of rigidity "k", which was related to the rigidity of the supports at every node. In order to replicate the measured live-load response, the top of the deck nodes were assigned vertical springs with a stiffness of 175,130 kN/mm (1,000,000 kips/in.) and longitudinal springs with a stiffness of 175.1 kN/mm (1,000 kips/in.). At the bottom nodes of the abutments, springs with vertical stiffness of 10,510 kN/mm (60,000 kips/in.) and transverse stiffness of 88 kN/mm (500 kips/in.) were applied. The central pier was modeled with transverse and vertical springs of 880 kN/mm (5,000 kips/in.) and 17,510 kN/mm (100,000 kips/in.), respectively.

Figure 14 shows a typical comparison between the measured and predicted strain at the mid-span of girder G4 as the truck was driven along load path Y2. Overall, the finite-element strain data was within 5% of the measured strains. Similar comparisons were made with other girders and load paths to validate that the finite-element model was accurately predicting the bridge response.

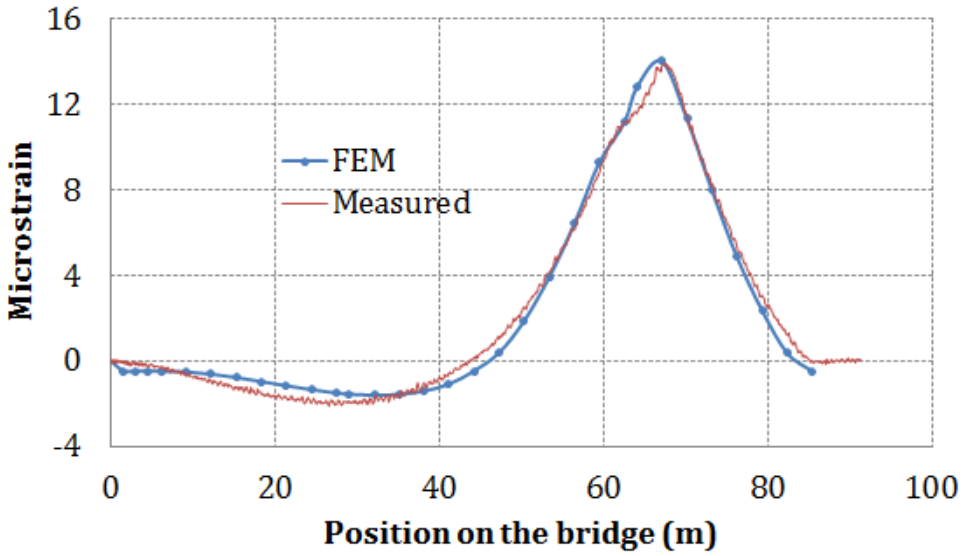

Figure 14 – Comparison between FEM vs. Live-Load Test Results – California Bridge.

Comparison of Tilt-meter vs. Data Measured

The Utah Bridge did not display the same end restraint as the California Bridge and measured temperature gradients and corresponding rotations were used to validate the model. In order to apply the measured temperature gradients in SAP2000, the temperature at every nodal location were input. This was accomplished by using the Joint Pattern Command in SAP. The joint pattern command allowed discrete temperatures to be input over the height and a linear interpolation was enforced between the nodes. Because of the dense temperature array on the deck, this resulted in a nearly parabola distribution over the height.

The observed boundaries conditions influenced the behavior of the structural response of the Utah Bridge since it was also built as an integral abutment bridge. Based on the observed behavior from a previous live-load test, the bridge was behaving very nearly a pinned type boundary condition. It is presumed that the cracking at the abutment contributed to the nearly restraint free end condition as such the bridge was modeled using pinned end conditions. Figure 15 shows a typical comparison of the measured rotations from the north side of Girder 2 and the finite-element model over a 24-hour time period. This figure shows a typical cyclical response as the bridge is heated during the day and then cooled at night. Overall, the magnitudes of the finite-element rotations were within 8% of the measured.

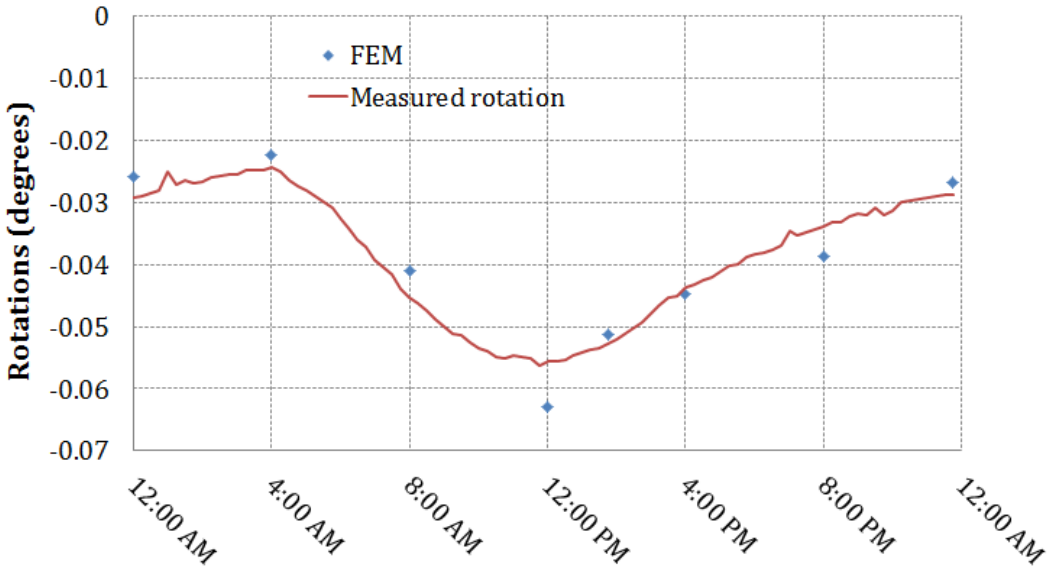

Figure 15 – Comparison between FEM vs. data measured – Utah Bridge.

A trend-line was fit between the measured and finite-element predicted rotations. The coefficient of correlation for this trend-line was found to have a value of 0.89, as shown in Figure 16. By having a strong correlation of rotation near the abutment, it was evident that the pinned boundary conditions at the abutment accurately predicted the bridge response due to changes in temperature gradients.

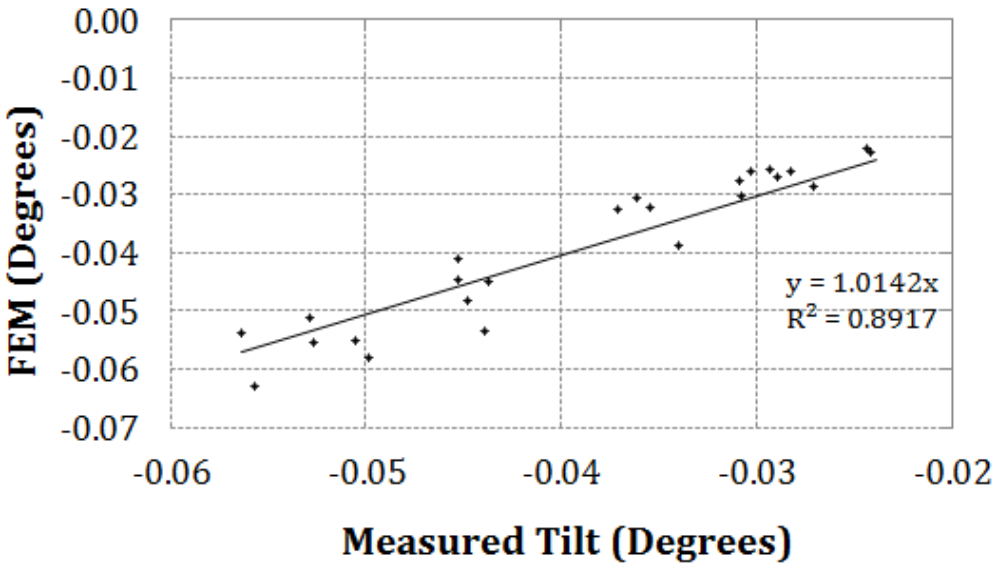

Figure 16 – Comparison between FEM vs. Measured tilt – Utah Bridge

Effects of temperature

Design Temperature Gradients Loading Case

Positive thermal design gradients from the AASHTO LRFD Bridge Design Specifications (2010) in addition to that recommended Priestley (1978) were also applied as load cases within the validated SAP2000 models and corresponding and corresponding stresses were calculated. Individual temperatures corresponding to the design gradient were also assigned to all the nodes on the model. The temperature between each nodal location was linearly interpolated. The models were used to not only illustrate internal stresses due to temperature gradients but also to study the effect of boundary conditions.

As previously discussed, large temperatures gradients can produce regions of tensile stresses over the cross section of the bridges due to the non-linear temperature gradient as well as due to any secondary effects from continuity. Thus, for the maximum positive gradient load case on a simply supported beam, compressive forces are produced at the top and bottom faces of the bridge's cross section and high tensile regions are created across the web of the bridge girder (Barr et al. 2005). For continuous beams, secondary moments are developed which can result in compressive stress at the top and tensile stresses in the web and bottom of the girder.

For comparison, the calculated temperature stresses can be compared with the modulus of rupture (f_r) for concrete. For these cases, AASHTO LRFD recommends using:

$$f_r = 0.62\sqrt{f_c'}(MPa) \quad or \quad f_r = 0.23\sqrt{f_c'}(ksi) \tag{2}$$

For the California Bridge (a two span continuous bridge with significant end restraint), the thermally induced stresses consisted of two components: one component caused by the nonlinear temperature gradient provided by the code and acting over the cross section, and another component due to the internal or secondary moments because of its continuous nature. For this bridge, two different boundaries conditions were applied: one with translational springs with provided stiffness at both ends and the center pier (validated model), and with pinned restraint on the north abutment and simple restraints on the south abutment and center pier. Figure 17 shows the relative cross section of the bridge end the corresponding predicted design stress profiles for the bridge with different boundaries conditions, corresponding to the maximum code specified positive measured temperature gradient for a concrete superstructure that is 400 mm (16 in.) or more in depth and located in Zone 1. For this figure, tensile stresses are considered positive.

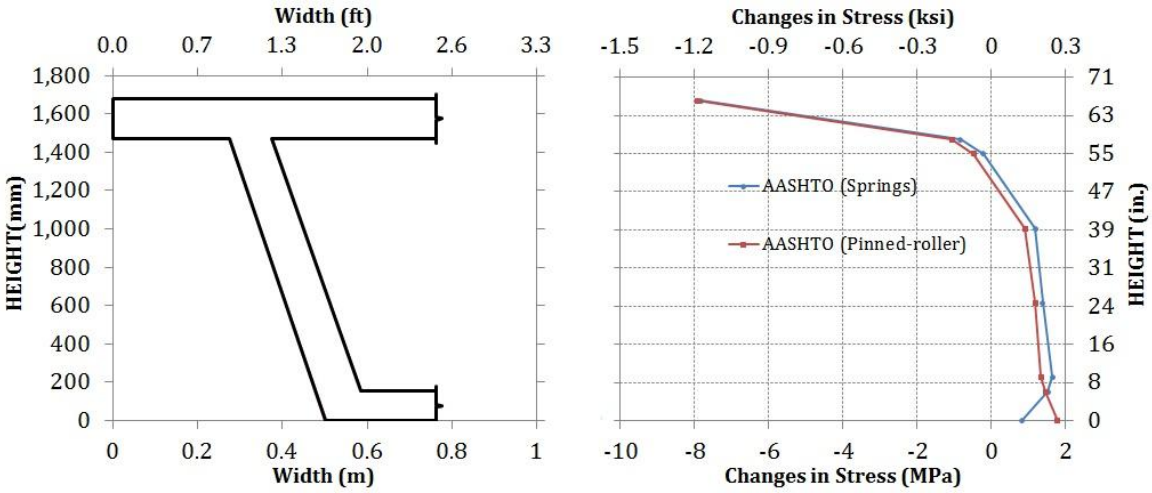

Figure 17 – Stress profile over the cross section of the California Bridge

The stresses for the as-is bridge condition (validated FE Model) were within 18% of the results of the pinned-roller boundary condition showing that the boundary conditions due influence the integral stresses. The maximum compressive stress at the top was 7.8 MPa (1,130 psi) for the as-is bridge condition. In comparison, the maximum compressive stress at the top was 8.2 MPa (1,190 psi) for the pinned-roller end condition. The maximum tensile stresses were found to be 1.65 and 1.85 MPa (240 and 265 psi), respectively, for the as-is and pinned-roller end conditions. These tensile stresses represent 59% of the allowable or direct tensile stress of a structure with a specified concrete compressive strength (f'_c) of 24.1 MPa (3,500 psi) as per AASHTO LRFD Specifications. Figure 28 located in Appendix 3 show the effect of the maximum temperature gradient when applied to the bridge model.

For the Utah Bridge (simply supported support conditions), the thermally induced stresses consisted of only one component caused by the nonlinear temperature gradient. Figure 18 shows the predicted design stress profiles for the bridge, corresponding to the maximum positive measured temperature gradient and the maximum AASHTO's gradient for a concrete superstructure that is 400 mm (16 in.) or more in depth and located in Zone 1. As before in this figure, tensile stresses are considered positive. Figure 29 located in Appendix 3 show the effect of the maximum AASHTO temperature gradient when applied to the bridge model.

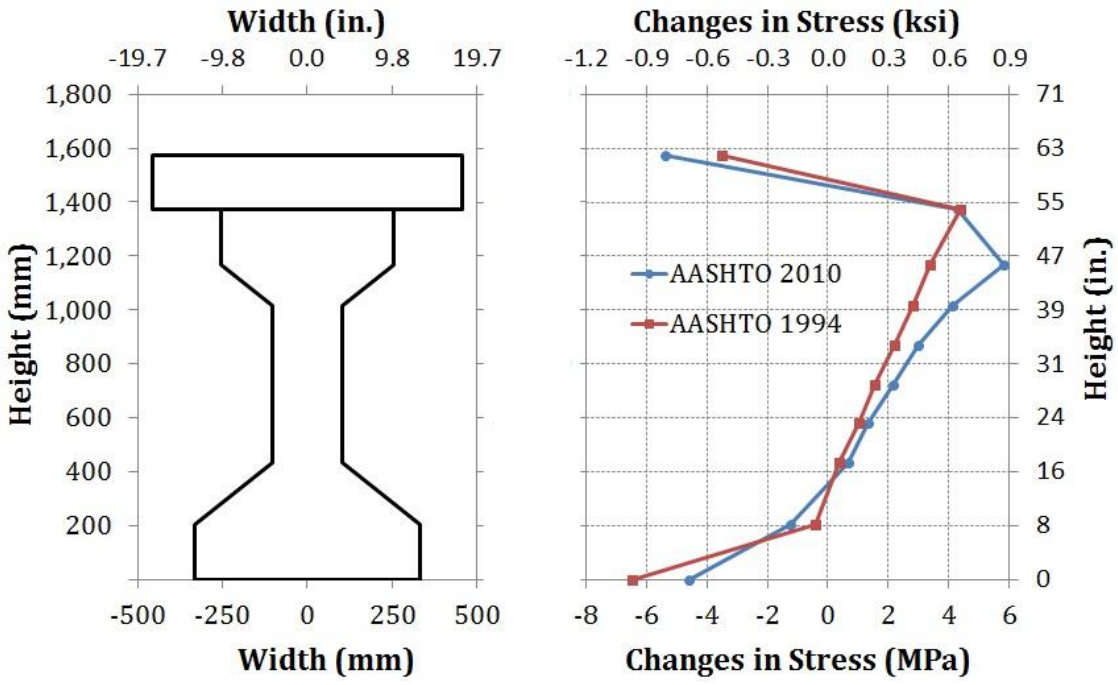

Figure 18 – Stress profile over the cross section of the Utah Bridge

The maximum compressive stresses at the top and bottom were 5.4 and 4.6 MPa (840 and 665 psi) for the AASHTO's temperature gradient, respectively. The maximum compressive stresses at the top and bottom were 6.7 and 3.6 MPa (970 and 530 psi), respectively, for the maximum measured positive gradient. The maximum tensile stresses were 5.8 and 4.5 MPa (850 and 660 psi) for the AASHTO and maximum measured positive gradients, respectively. The average tensile stresses exceeded by 65% the allowable or direct tensile stress of a structure with a specified concrete compressive strength (f'_c) of 27.6 MPa (4,000 psi) as per AASHTO LRFD Specifications. This type of tensile overstressing of the structure is a potential cause of the cracking, especially at the abutments and under the parapets, as shown in Figure 30-Figure 32 located in Appendix 3.

As previously mentioned, the AASHTO's current temperature gradient does not take into consideration the possible insulation effect caused by the asphalt overlay. An average difference of 33.5% was found between the stresses caused by the AASHTO Specifications (1994) and AASHTO's temperature gradients demonstrating that the asphalt can play an important role in reducing the magnitude of the temperature gradients the bridge superstructure over its service life.

CHAPTER 4

SUMMARY AND CONCLUSIONS

Summary

As part of a study to quantify temperature effects on bridges, field instrumentation was installed and monitoring was performed on an integral abutment bridge located in California and Utah. These bridges were subjected to an initial live load test to validate a finite-element model and subsequently monitored for changes in temperatures over the height of the superstructure to evaluate the effect that temperature stress cause on integral abutment bridges.

A comprehensive instrumentation plan was prepared to provide continuous evaluation and structural health monitoring of both the California and Utah bridges. Seasonal and daily temperature variations were measured using two different types of sensors: tilt-meters and thermocouples. Since bridge temperatures have been found to vary over the bridge cross section as a function of time, daily maximum and minimum average temperature variations were measured for the California and Utah Bridges and compared to the temperature ranges provided in the AASHTO LRFD Bridge Design Specifications (2010). Minimum values of T_{avg} occurred in the early morning hours of the coldest nights, and maximum values of T_{avg} occurred in mid-afternoon of the hottest days.

Also, daily variations in the maximum positive and negative temperature gradient were recorded in order to quantify changes in stress over the height of the cross-section of the bridges and their corresponding end rotations. To accomplish that, two finite-element models were created for the California and Utah Bridges and calibrated using data obtained from live-load tests and measured temperatures.

For the California Bridge, the live-load test consisted of driving two trucks at approximately 8 km/hr (5 mph) along the length of the bridge. Changes in strain and rotations were recorded along five selected load paths. This data was used to validate a detailed finite-element model using solid elements. Furthermore, additional model validation was performed with daily measurements of the concrete temperatures and corresponding end rotations. For the Utah Bridge, the finite-element model was also validated using measured temperature gradients and end rotations. The installed instrumentation provided excellent data concerning the distribution of temperatures across the cross-section and end rotations at the abutments.

Using these calibrated finite-element models and the maximum measured temperatures gradients, the effect of end restraint and an asphalt overlay were quantified.

Conclusions

The measured changes in temperature and rotation were used with the finite-element models of both bridges to quantify bridge behavior and validate code-based procedures. Based on the findings, several conclusions were obtained.

1. The AASHTO LRFD (2010) design recommendations for the maximum and minimum average temperatures of the California and Utah Bridges were predicted with 17 and 27%, respectively. The measured bridges data indicated average temperatures that were well within the design limits for Region 1. Extreme summertime high temperatures and extreme wintertime low temperatures clearly approached the design limits during summer and winter extremes, in some cases a slight difference of 3 ˚C (6.5 ˚F).
2. The maximum positive and negative gradients were compared to ASSHTO LRFD Specifications and other studies. For the California and Utah Bridges, the maximum measured positive and negative gradients were perfectly encompassed by the AASHTO LRFD Codes and Priestley's gradient but with a significant difference at the bottom gradient which was underestimated by at least two times their values. In general, the AASHTO LRFD gradients predicted the gradient more accurately than Priestley distribution, but for the Utah Bridge, AASHTO's gradient greatly overestimated the measured temperature gradients which can be an indication of a thermal isolation effect provided by the asphalt overlay.

3. For the California Bridge, a live-load test was used to validate the model since very small rotations were obtained when the temperature gradients were applied; not being the same for the Utah Bridge, which measured temperature gradients and corresponding rotations were used to validate the model. Overall, finite-element models accurately predicted the bridges response within 5 and 8% of the measured data.
4. For the California Bridge, a reduction of 18% was obtained comparing the stresses of the validated finite-element model (partially restrained) and the assumed design condition of pinned-roller end restraint. The maximum tensile stresses calculated for the California Bridge represented 59% of the allowable or direct tensile stress of a structure as per AASHTO LRFD Specifications (2010).
5. For the Utah Bridge, it was found that an average difference of 33.5% existed between the calculated stresses caused by the maximum measured gradients and AASHTO's temperature gradients. This difference was primarily believed to be a result of the smaller measured temperature gradients due to the four inch asphalt overlay. This finding illustrates that the asphalt overlay effectively reduced the magnitude of the temperature gradients on the bridge. The influence of the asphalt overlay is not currently taken into account in the AASHTO Specifications. The measured temperature gradient produced high tensile stresses (850 and 660 psi) that exceeded by a significant percentage (60%) of the allowable or direct tensile stress of a structure. This finding supports the idea that severe damage or failure can

occur on bridge superstructures due to thermal effect or not producing appropriate detailing. In the case of the Utah Bridge, these stresses could have been the cause of the bridge abutments and parapets to cracking.

REFERENCES

AASHTO. (1994). *AASHTO LRFD Bridge Design Specifications,* 1st Ed., Washington, D.C.: American Association of State Highway and Transportation Officials (AASHTO).

AASHTO. (1996). *AASHTO Standard Specification for Highway Bridges,* 15th Ed., Washington, D.C.: American Association of State Highway and Transportation Officials (AASHTO).

AASHTO. (1998). *AASHTO LRFD Bridge Design Specifications,* 2nd Ed., Washington, D.C.: American Association of State Highway and Transportation Officials (AASHTO).

AASHTO. (2010). *AASHTO LRFD Bridge Design Specifications,* 4th Ed., Washington, D.C.: American Association of State Highway and Transportation Officials (AASHTO).

Barr, P. J., Stanton, J. F., & Eberhard, M. O. (2005). Effects of Temperature Variations on Precast, Prestressed Concrete Bridge Girders. *ASCE - Journal of Bridge Engineering, Vol. 10, No. 2*, 186-194.

Branco, F., & Mende, P. (1993). Thermal Actions for Concrete Bridge Design. *ASCE - Journal of Structural Engineering, Vol. 119, No.8*, 2313-2331.

Computers and Structures, I. (2011). SAP2000, Version 15 Analysis reference.

Elbadry, M., & Ghali, A. (1986). Thermal Stresses and Cracking of Concrete Bridges. *American Concrete Institute (ACI) Journal*, 1001-1009.

Emerson, M. (1982). *Thermal movements of concrete bridges: field measurements.* Crowthorne, England: Transport and Road Research Laboratory.

Imbsen, R. (1985). *Thermal Effects in Concrete Bridge Superstructures.* Washington, D.C.: NCHRP 276. Transportation Research Board.

Leonhardt, F. (1970). Lessons from Damage to Prestressed Concrete Bridges. *Beton-und Stahlbetonbau (German)*, 231-244.

Moorty, S., & Roeder, C. W. (1990). Thermal response of skewed bridges. *Developments in short and medium span bridge engineering. Canadian Society of Civil Engineers*, 343-353.

Moorty, S., & Roeder, C. W. (1992-April). Temperature Dependent Bridge Movements. *ASCE - Journal of Structural Engineering*, 1090-1105.

Priestley, M. (1978). Design of concrete bridges for temperature gradients. *American Concrete Institute (ACI)*.

Priestley, M., Thurston, S., & Cooke, N. (August 1984). Influence of cracking on thermal response reinforced concrete bridges. *Concrete International*, 36-43.

Roeder, C. W. (2002). *Thermal Movement Design Procedure for Steel and Concrete Bridges.* Seattle, WA: National Cooperative Highway Research Program (NCHRP 20-07/106).

Roeder, C. W. (2003). Proposed Design Method for Thermal Bridge Movements. *ASCE - Journal of Bridge Engineering*, 12-19.

Thepchatri, T., & Johnson, C. P. (1977). *Prediction of Temperature and Stresses in Highway Bridges by a Numerical Procedure using Daily Weather Reports (FHWATX-*

77-23-1). Austin, Texas: Center for Highway Research of The University of Texas at Austin.

APPENDICES

APPENDIX 1. Bridges description

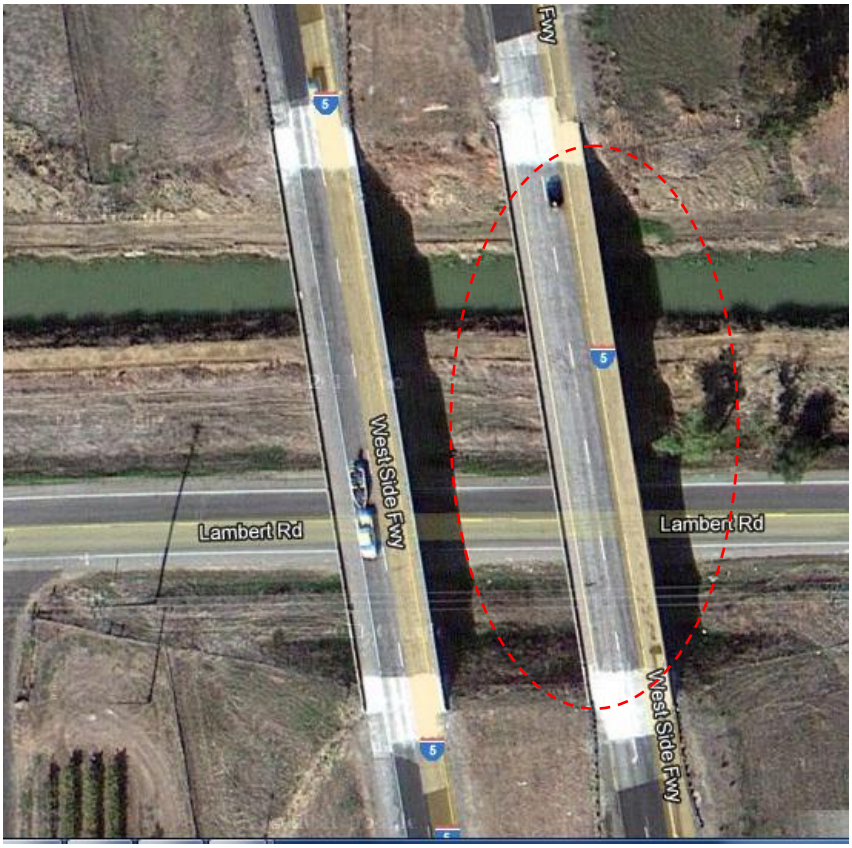

Figure 19 – Aerial view of California Bridge.

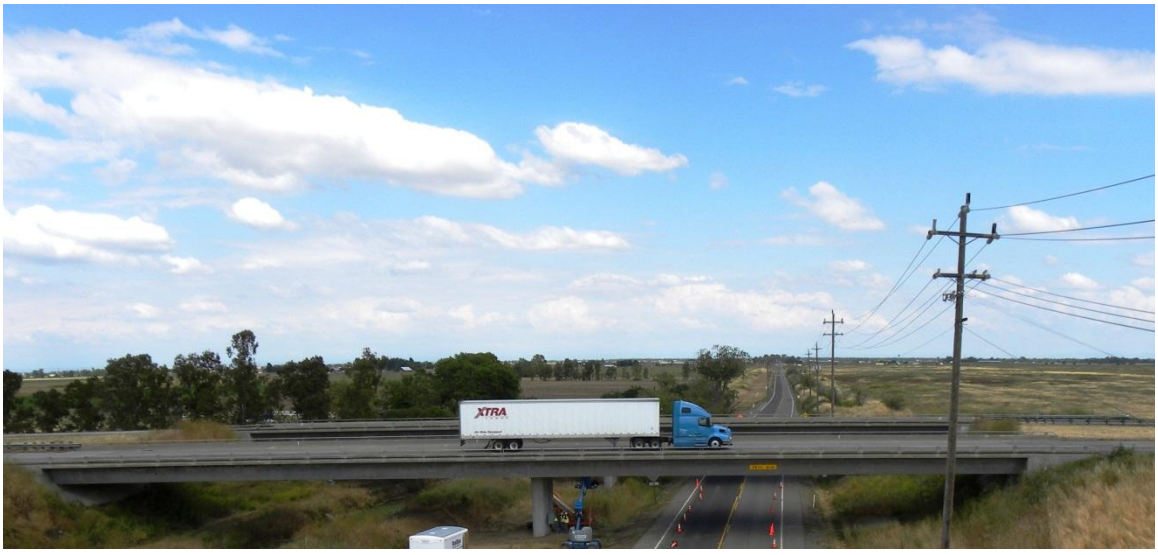

Figure 20 – California Bridge part of Interstate-5 (I-5) over Lambert Road.

Figure 21 – Aerial view of the Utah Bridge.

Figure 22 – Utah Bridge part of Interstate-15 (I-15) over Cannery Road.

APPENDIX 2. Bridge Instrumentation

Figure 23 – Deck Thermocouples installed in the California Bridge.

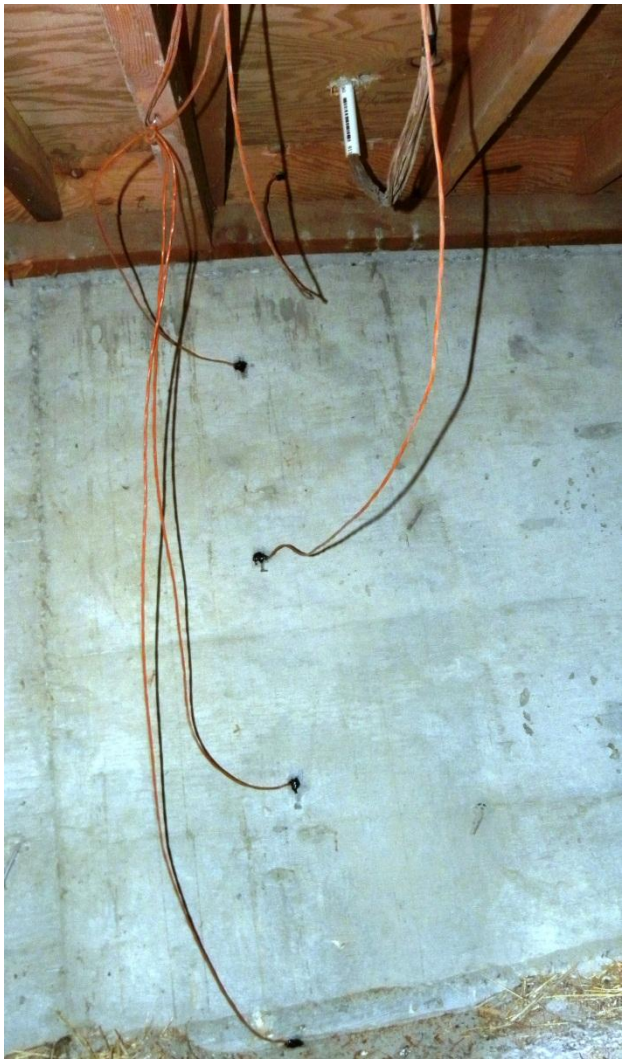

Figure 24 – Deck and Web thermocouples installed in the California Bridge.

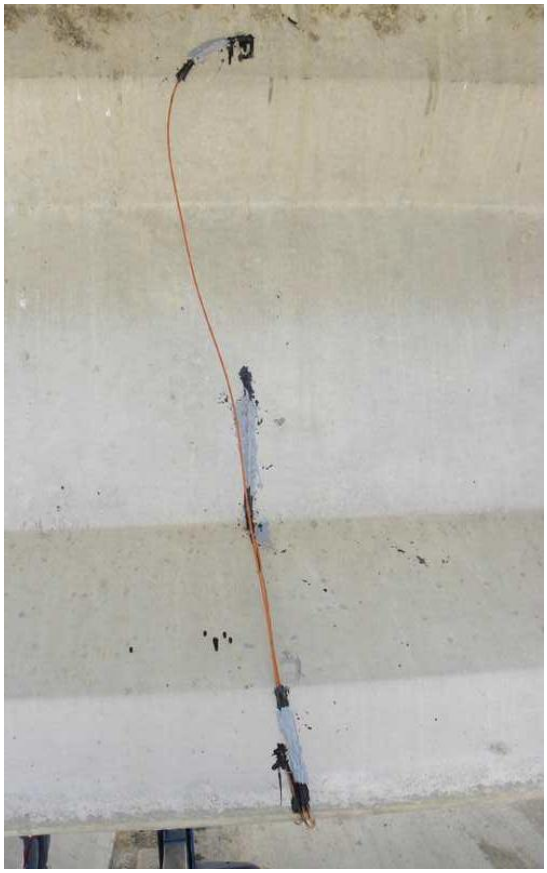

Figure 25 –Web thermocouples installed in the Utah Bridge.

Figure 26 – Deck thermocouples installed in the Utah Bridge.

Figure 27 – Weather Station installed near the Utah Bridge.

APPENDIX 3. Effects of Temperature

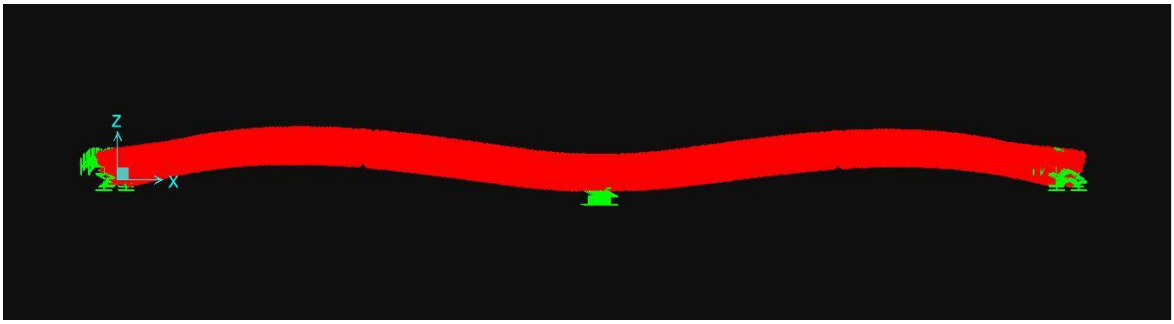

Figure 28 – Effect of maximum temperature gradient on the California Bridge modeled in SAP2000.

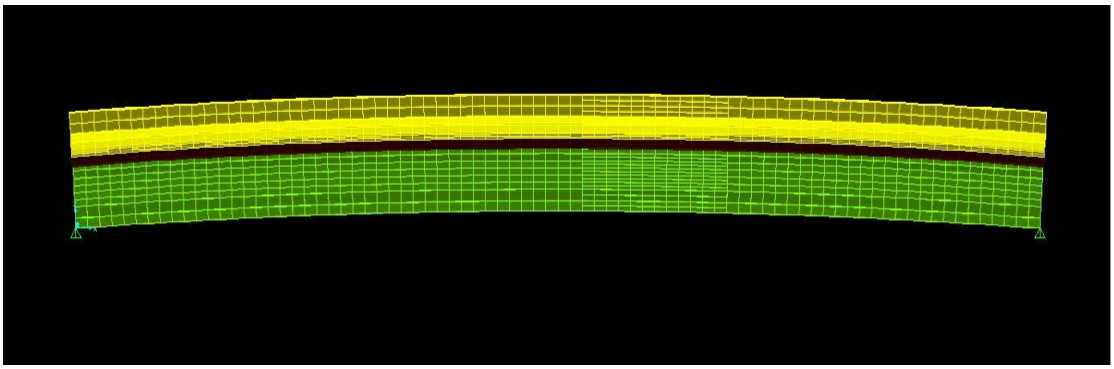

Figure 29 – Effect of maximum temperature gradient on the Utah Bridge modeled in SAP2000.

Figure 30– Cracking at the abutment on the Utah Bridge.

Figure 31 – Cracking at the abutment on the Utah Bridge.

Figure 32 – Cracking at parapets on the Utah Bridge.